Summer 2017

Sedimentary Characteristics and Nutrient Sequestration of Embanked Floodplains Along the Lower Mississippi River, Mississippi and Louisiana

R M Malitha Rathnayake
University of Southern Mississippi

SEDIMENTARY CHARACTERISTICS AND NUTRIENT SEQUESTRATION OF EMBANKED FLOODPLAINS ALONG THE LOWER MISSISSIPPI RIVER, MISSISSIPPI AND LOUISIANA

by

R M Malitha Rathnayake

A Thesis
Submitted to the Graduate School,
the College of Science and Technology,
and the Department of Geography and Geology
at The University of Southern Mississippi
in Partial Fulfillment of the Requirements
for the Degree of Master of Science

August 2017

SEDIMENTARY CHARACTERISTICS AND NUTRIENT SEQUESTRATION

OF EMBANKED FLOODPLAINS ALONG THE LOWER

MISSISSIPPI RIVER, MISSISSIPPI AND LOUISIANA

by R M Malitha Rathnayake

August 2017

Approved by:

_____

Dr Franklin Heitmuller, Committee Chair
Associate Professor, Geography and Geology

_____

Dr Jeremy Deans, Committee Member
Assistant Professor, Geography and Geology

_____

Dr Paul F. Hudson, Committee Member
Associate Professor, Geography and Geology

_____

Dr Kevin A. Kuehn, Committee Member
Professor, Biological Sciences

_____

Dr Mark Puckett
Chair, Department of Geography and Geology

_____

Dr. Karen S. Coats
Dean of the Graduate School

Published by the Graduate School

THE UNIVERSITY OF SOUTHERN MISSISSIPPI®

ABSTRACT

SEDIMENTARY CHARACTERISTICS AND NUTRIENT SEQUESTRATION OF EMBANKED FLOODPLAINS ALONG THE LOWER MISSISSIPPI RIVER, MISSISSIPPI AND LOUISIANA

by R M Malitha Rathnayake

August 2017

The Mississippi River Basin is the largest river basin in North America and the third largest river basin in the world. Most of the corn, soybeans, wheat, cattle, and hogs harvested in the United States come from the Mississippi River Basin and about 58% of the entire drainage basin is croplands. Runoff from these lands carries sediments and nutrients, and the Mississippi River transports these downstream and ultimately deposits them in the Gulf of Mexico. The northern Gulf of Mexico is one of largest human-caused hypoxic zones in the world. Hypoxia is the phenomena where the dissolved oxygen level decreases in the water because of the eutrophication. Nutrients, particularly nitrogen (N) and phosphorus (P) are the main causes of eutrophication and the Mississippi River is the main source for nutrients in the Gulf of Mexico. The lower Mississippi River is frequently subjected to flooding during high discharge and floodwater sediments and nutrients are introduced into the floodplain. This study hypotheses that considerable concentration of nutrients are sequestrated in the Lower Mississippi Floodplain and the sequestration patterns are different in different sub-fluvial environments. Eight sediment cores recovered from three different sub-environments including levee backslope, point-bar and backswamp, taken from the Lower Mississippi floodplain were analyzed for their organic matter (OM), carbon (C), nitrogen (N), phosphorus (P), magnetic susceptibility,

and particle size with depth. High concentrations of C, N, and OM are decreasing with depth and become low and relatively constant concentrations at depth no more than 25 cm. Levee backslope sediments consist of high silt and sand size particles, and have low concentration of C, N and OM. Backswamps and point-bar sediments are rich in clay size particles, C, N, and OM. C and N in the studied sediment samples were mainly originated from OM and total P is mainly from inorganic sources. Average concentration values in the topsoil for three sub-environments show moderate C and N concentrations and significantly high P concentrations compared to previous studies carried out in similar environments. Depth and OM concentration are the main factors governing the C and N concentrations while depth and clay fraction is more important in determining P concentrations. Results of this study show that floodplains are served as a sink for removing nutrients from further downstream movement effectively. Further study should be completed to understand the temporal changes in nutrient sequestration of the study area in order to quantify the amount of nutrients sequestrated within the floodplain.

ACKNOWLEDGMENTS

It is a great pleasure to thank all those who have contributed to my research work to become a success. Foremost, I gratefully acknowledge my advisor Dr. Frank Heitmuller who gave the great support, encouragement, mentorship, and motivation throughout the research as well as last two years of my stay at The University of Southern Mississippi. I would also like to offer my sincere thanks to Dr. Mark Puckett, Chair of the Department of Geography and Geology, for the enthusiastic support to complete the research. I wish to extend my gratitude to Dr. Paul Hudson for his valuable time and constant encouragement during the entire research beginning with the sample collection phase. I also grateful to the committee members, Dr. Jeremy Deans and Dr. Kevin Kuehn, for their support. I am also thankful to Dr. Jake Schaefer for helping me with the statistical analysis. I also convey my gratitude to the faculty and staff of the Department of Geography and Geology, including Dr. Andy Reese for access to his laboratory.

It is a great pleasure to thank graduate students of the Geology program, James Thompson, Daniel Winkler, David Simmons, and Theresa Woehnker for their support and encouragement. All the members from the Dr. Kuehn's microbial ecology lab, Department of Biological Sciences, are also acknowledged for their support. Of notable mention include Dr Halvor Halverson, Matthew Lodato, and Tori Hebert for their constructive suggestions and help. Additionally, I thank personnel at the U.S. Fish and Wildlife Service for a research permit, housing, and logistical advice during the data collection trip.

Finally, I would like to thank my loving parents, wife, sister and friends. You are my strength, my pride and my belief. Thank you very much for your hand being always with me.

TABLE OF CONTENTS

LIST OF TABLES

LIST OF ILLUSTRATIONS

CHAPTER I - INTRODUCTION

The Mississippi River Basin includes the largest drainage area in North America and is the third largest river basin in the world. Only the Amazon River in South America and the Congo River in Africa have larger drainage areas than the Mississippi River. The Mississippi River is one of the most productive agricultural regions in the world and about 58% of the drainage area is cropland (U.S Geological Survey, 2000). Most of the corn, soybeans, wheat, cattle, and hogs harvested in the United States are coming from the Mississippi River Basin. Runoff from these lands delivers suspended sediments, naturally occurring chemicals as a result of chemical weathering, and unnaturally occurring contaminants such as nutrients and pesticides. The Mississippi River plays a main role in transporting these sediments and nutrients downstream and ultimately discharging them into the Gulf of Mexico.

The Mississippi River is considered one of the most regulated rivers in the world. During the 20th century, many structures have been built along the river and its tributaries, including dams and reservoirs, artificial levees, dikes, and concrete revetments, which can greatly influence sediment delivery and sedimentation along the floodplain and channel of the Mississippi River (Hudson et al., 2008). In addition to structures, river shortening and channelization also have been done between 1929 and 1942 to improve and maintain navigation (Kesel, 2003). As a result, the Mississippi River was shortened by 245 km and between 1939 and 1955 the river was shortened by an additional 88 km. As a cumulative result of these modifications, both sediment loads and channel-floodplain connectivity have been greatly reduced. Dam and reservoir construction during the 1950s and 1960s on major tributaries like the Missouri and

Arkansas Rivers alone accounted for 50% to 70% reduction of suspended sediment reaching the Gulf of Mexico (Meade and Moody, 2010). Horowitz (2010) concluded that the reduction in sediment supply throughout the Mississippi River Basin has been caused by the insertion of numerous engineered structures in conjunction with the introduction of better land management practices to limit erosion. The 1993 flood contributed to this effect by flushing substantial quantities of stored, readily erodible, in-channel bed sediments from the basin.

Alongside the depletion of Mississippi River sediment to the Gulf of Mexico, other environmental problems associated with human activities in the Mississippi River Basin are well documented. Hypoxia is an environmental phenomenon where the concentration of dissolved oxygen decreases below a level of 2 ppm where living aquatic organisms can no longer survive. The northern Gulf of Mexico adjacent to the Mississippi River is considered the largest human-caused hypoxic zone in the United States (Rabalais et al., 2002). According to the National Oceanic and Atmospheric Administration (NOAA, 2017), the average size of the hypoxic zone in the northern Gulf of Mexico over the period between 1985–2005 is about 13,650 square kilometers. The reason for this hypoxic condition is eutrophication. Nutrients, particularly nitrogen (N) and phosphorus (P) provide favorable conditions for excessive algal growth, which utilize dissolved oxygen for respiration and decomposition. The Mississippi River transports most of these nutrients to the Gulf. Understand nutrient loads and reservoirs are important from an environmental management perspective. Nutrient sequestration along Lower Mississippi (LMR) embanked floodplains is an important process to consider because this serves as a sink to remove nutrients from further downstream transport, which would

potentially limit nutrients reaching the Gulf of Mexico. It is also important to understand at what depth of the soil column nutrients begin to degrade or leach out into shallow groundwater tables.

Efforts within the LMR alluvial valley to invigorate ecosystems through channel-floodplain connectivity are complicated by the presence of flood-control levees and inundation patterns along the embanked floodplain corridor (Hudson et al., 2008). A variety of ecosystem services are afforded when high flows along the river are connected to floodplain environments through sloughs and crevasses; including access to spawning habitats for selected fish species, maintenance of aquatic riparian habitats such as oxbow lakes, and enhancement of riparian habitat diversity (Sparks, 1995; Ward and Stanford, 1995; King and Keeland, 1999; Miranda, 2005; Zeug and Winemiller, 2008; Phelps et al., 2015). Further, larger floods completely inundate the embanked floodplain resulting in a suite of different ecosystem services, including but not limited to, seed dispersal, downstream flood attenuation, alluvial aquifer recharge, sediment deposition, and contaminant and nutrient sequestration (Craft and Casey, 2000; Mitsch et al., 2001; Battaglia et al., 2002; Tockner and Stanford, 2002; Schramm et al., 2009; Zehetner et al., 2009; Acreman and Holden, 2013).

This study will focus on the embanked LMR floodplain, which only experiences flooding during high discharge events. Despite the extensive research focused on the sources of sediment and anthropogenic sources of nutrients to river systems and their ultimate delivery to coastal waters (U.S Geological Survey, 2000; Rabalais et al., 2002; Goolsby et al., 1999), far less is known about long-term nutrient sequestration in floodplain sediments and the potential of sedimentation along the Mississippi River

floodplains that interrupt downstream transport to the coastal zone. Understanding the processes involved in floodplain sedimentation is important to understand geomorphic variability and river management strategies in large alluvial valleys because sediment and nutrient budgets of a river basin are heavily dependent upon floodplain sedimentation (Schramm et al., 2009) and can help reduce large human-made hypoxic zones.

This study examines sediments from eight different cores along the LMR floodplain; including properties such as particle size, magnetic susceptibility, and organic matter and nutrient contents (N, P, and C). An attempt is made to discuss the variations of the above parameters with depth, position relative to the channel, and depositional sub-environments.

1.1 RESEARCH QUESTIONS

This study focuses on answering three main primary research questions:

(i) How do sedimentary characteristics such as particle size, organic matter content and sediment composition, vary with depth in different depositional sub-environments of the embanked alluvial floodplain?

(ii) How do nutrient concentrations vary with the depths and what are the approximate depths that nutrients are sequestered in the LMR alluvial floodplain before they are degraded to end products or removed via leaching?

(iii) How do depositional characteristics such as particle size, organic matter, mineral composition (magnetic susceptibility as a surrogate), distance from the main river and other characteristics affect concentrations of nutrient sequestration in the LMR alluvial floodplain?

1.2 HYPOTHESES

Main hypothesis of this study are:

(i) Sedimentary characteristics (Particle size, organic content and sediment composition) vary with depth in different depositional sub-environments such as backswamps, point-bars, and levees.

(ii) Considerable sequestration of nutrients occurs in these sediments, but nutrients substantially decrease (degrade) at a certain depth.

(iii) Nutrient sequestration is greatly influenced by the distance from the main channel, the particle size of the sediments, organic matter content, and general mineral composition (magnetic susceptibility as a surrogate).

(iv) Trends in nutrient sequestration patterns may have a correlation with structures built upstream because differences of sequestered nutrient concentrations can be related to how the nature of sedimentation has changed through time.

CHAPTER II - LITERATURE SURVEY

2.1 ALLUVIAL FLOODPLAINS AND SEDIMENTATION

An alluvial floodplain deposits consist of sediments that have been deposited by a river or a stream. Overbank sediments are deposited by flood waters that have breached or overtopped the banks. Overbank areas are associated with channels of all types, including the frequently flooded Lower Mississippi alluvial floodplain. Overbank areas can be divided into: (i) proximal areas close to active channels (levees and crevasse splays), (ii) distal areas at some distance from a channel (backswamps), and (iii) meander scrolls (ridges and swales) and abandoned channels in proximal and distal zones (figure 2.1).

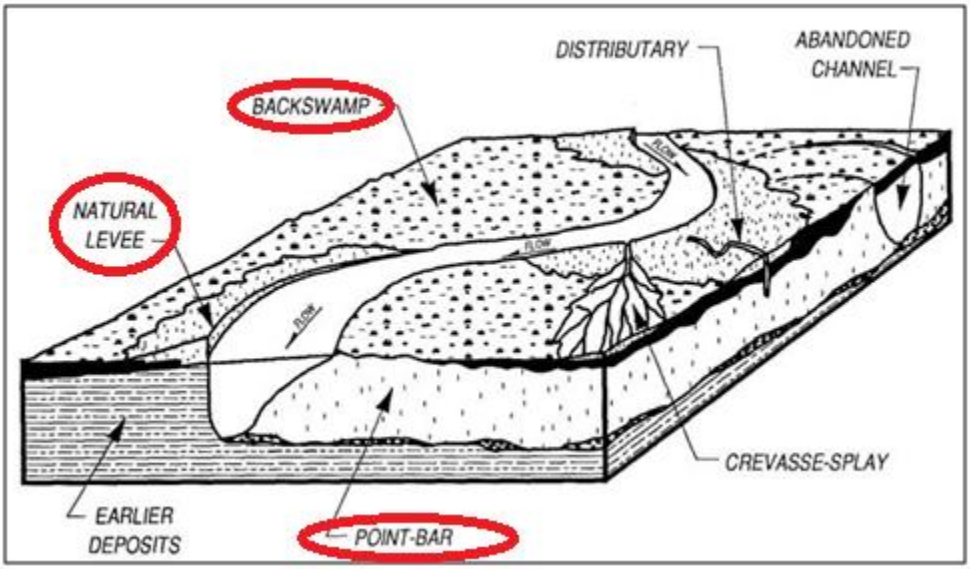

Figure 2.1 Floodplain depositional sub-environments in a meandering river system.

(modified from Saucier, 1994).

2.1.1 Floodplains and Backswamps

A floodplain is the area of land adjacent to a river that stretches from the banks of its channel to the base of the enclosing valley walls. Floodplains experience frequent flooding during periods of high discharge. Many areas in temperate and tropical floodplains are intensely cultivated and thus disturbing the natural flow, erosion, and deposition of the river system. Although wind-blown dust can be an important agent of deposition in certain regions, suspended sediments during floods are the primary source of floodplain accretion. Flooding in floodplains can occur from either overtopping floodwater from the river channel or from a rise of the water table and the formation of floodplain lakes (Collinson, 1996). Flooding can occur from intense precipitation on the floodplain or from high stages along the river. When floods occur as a direct result of overtopping along major river channels, the grain size of floodplain sediments tends to decrease distally (Kesel et al., 1974; Guccione, 1993; Saucier, 1994; Hudson and Heitmuller, 2003). Between floods, floodplains commonly dry out but in some places where the river flows close to its base level, floodplain sediments may remain saturated with water like in swamps and lakes. A backswamp is a depressed area of a floodplain between levees and the edge of the floodplain. Backswamp deposits consist of fine silt and clay resulting from settling of muddy water after a flooding event (Farrell, 1987). If flow is established on the floodplain between lakes or close to river channels, localized erosion can lead to a reworking of earlier floodplain sediments (Nanson and Croke, 1992; Heitmuller et al., 2017).

2.1.2 Levees and Crevasse Splays

Levees are ridges higher than both the channel and the surrounding floodplains. Levees are deposited on either side of a channel but commonly are better developed on the outer margins of meander bends (Hudson and Heitmuller, 2003). Levees grow through the deposition of suspended sediment during submergence by major floods. During lesser floods, they may be the only dry land on the floodplain. Sediment grain sizes commonly become finer away from the channel as floodwater overtop levees, turbulence diminishes, and suspended sediment is deposited (Kolb, 1962; Cazanacli and Smith, 1998). Levee deposits are mainly fine-grained sands and silts dominated by ripple-cross lamination and small-scale cross bedding (Singh, 1972). Bioturbation can disrupt or destroy the lamination.

A crevasse splay is a sedimentary deposit that forms when a stream breaks through natural or artificial levees and deposits sediment on a floodplain. A crevasse splay deposit is similar in pattern to an alluvial fan deposit. As the water spreads into the floodplain sediments will start to fall out of suspension as the water loses energy. Further, from the channel, isolated crevasse splays may be interbedded with fine-grained backswamp deposits and discrete sand beds (Farrell, 1987).

2.1.3 Point Bars

Point bars are common depositional features associated with matured meandering rivers. Point bars develop on the convex side of meander bends along meandering, mixed-load channels and accrete laterally as the meander bend migrates with both downstream and transverse components of movement (Bernard and Major, 1963). Because of the lateral movement of meanders coupled with the episodic development of

chute cutoffs, an asymmetrical ridge and swale topography will develop on the inside of the bends and create successive meander scroll patterns. Point bar deposits are generally characterized by a fining upward sequence from gravel-lag deposits to cross-bedded sands to a fine-grained drape at the very top (Saucier, 1994). Generally, the grain size of the point bar deposit is a reflection of the river's competence.

2.2 LOWER MISSISSIPPI ALLUVIAL VALLEY

The Lower Mississippi alluvial valley (LMAV) extends over a distance of about 780 km from the confluence of Mississippi and the Ohio rivers to the Gulf of Mexico (Figure 2.2). The eastern boundary of LMAV is well defined along distinct bluffs separating the valley from dissected coastal plains of Tertiary age (Figure 2.2). Principal tributary valleys merge with the main Mississippi Valley and make it difficult to identify the western boundary of LMAV (Saucier, 1994). Fisk (1944) identified the Mississippi alluvial valley as that area characterized by landforms and deposits resulting from the Last Glacial Maximum. Fisk (1944) recognized the Holocene alluvial plain and several older uplands within the alluvial valley. Those Holocene-age areas, which are subject to flooding by the present hydrologic regime, such as the Mississippi meander belt, were defined as the alluvial plain and uplands areas including those of Tertiary age (e.g., Crowley's Ridge) as well as braided stream terraces (e.g., Macon Ridge). Consequently, the LMAV is defined based on chronologic rather than geomorphic criteria (Saucier, 1994). As a solution to this nomenclature problem, landforms and sedimentary deposits that are primarily of Wisconsin and Holocene age are considered as the Lower Mississippi Valley (Saucier, 1994). The alluvial plain and the deltaic plain are the two

main distinctive geomorphic subdivisions of the Holocene Lower Mississippi Valley (Autin et al., 1991).

The width of the lowland containing late Wisconsin and Holocene sediments ranges from about 80 - 200 km (Knox, 2007) and the deltaic plain extends about 240 km in both east-west and north-south directions. The alluvial valley has an area about 86,000 km^2 and the deltaic plain area is about 40,000 km^2 (Saucier, 1994). The present floodplain is about 84 m above sea level at the upstream end near Cairo, Illinois, and about 12 m above sea level at the head of the deltaic plain (Autin et al., 1991; Saucier, 1994).

The upper two-thirds of the river from Cairo to Red River Landing, which is classified as the alluvial valley (Autin et al., 1991), consists of backswamps and meander belts (Hudson and Kesel, 2000). Meander belts include sinuous, active and abandoned channels, point bars with curved ridges and swales, and natural levee deposits. Backswamps are local depressions between meander belts and include freshwater swamps and crevasse-splay complexes (Aslan and Autin, 1999). Within the alluvial valley, Holocene age sediment deposits occupy only about 46 percent of the total area. The remaining 54 percent of the valley is characterized by braided stream terraces (valley trains) of Early and Late Wisconsin age. North of the latitude of Memphis, Tennessee, the alluvial valley is dominated by the valley trains and occur to a lesser extent as far as the Red River (Saucier, 1994). The river segment, downstream of Red River landing, flows through deltaic plain deposits. The ability of the river to laterally migrate is greatly reduced within the deltaic plains because of the presence of cohesive clays (Hudson and Kesel, 2000).

Based on upland Tertiary-aged remnants and terraces and ridges of Wisconsin and pre-Wisconsin age, Saucier (1994) subdivide the LMAV into six major lowlands or basins. These lowlands include the: Western lowlands, St. Francis basin, Yazoo basin, Arkansas lowland, Boeuf basin, and Tensas basin. All major basins that are bounded by Mississippi River meander belts consist of a definable topographic depression with bounding interfluves. In all cases, drainage is from north to south into a major collecting stream for which the basin is named (Saucier, 1994). In addition to lowlands, the LMAV includes several ridges such as Crowley's Ridge, Grand Prairie Ridge, and Macon Ridge. Even though these features are not considered as major divisions of the alluvial plain, they serve as important interfluves between major basins.

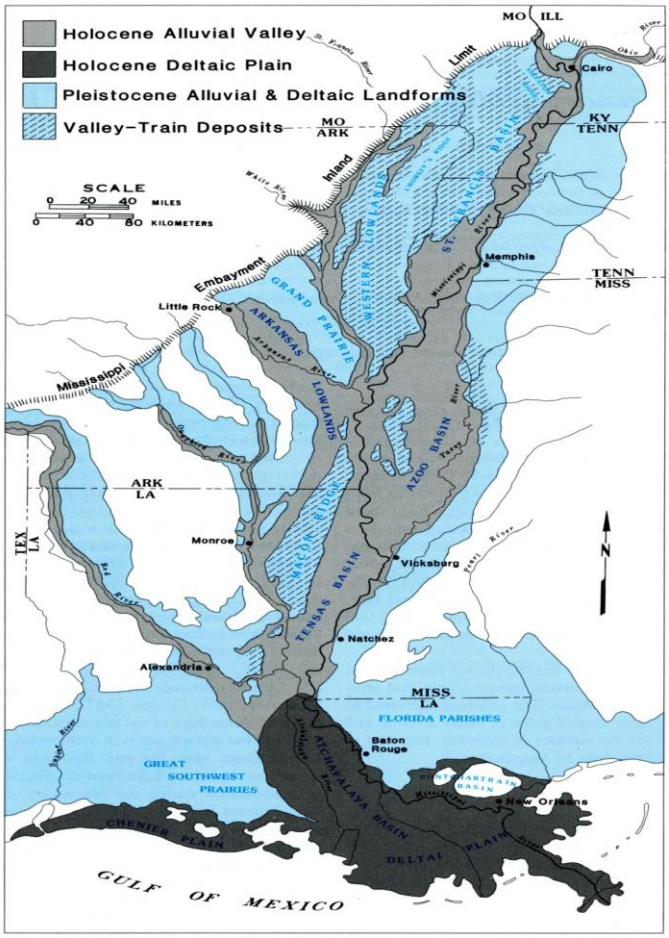

Figure 2.2 Lower Mississippi Alluvial Valley and the general location of the study area (modified from Aslan and Autin, 1991).

2.2.1 Fluvial geomorphology of the LMAV

The Lower Mississippi River (LMR) has led to erosion and deposition forming a broad spectrum of fluvial features for hundreds of thousands of years to produce the LMV. Because of the large extent of unconsolidated material and the humid climate that promotes chemical weathering, rates of erosion in the LMV region are considerably high (Saucier, 1994). A relatively low hydraulic gradient and high sediment concentrations transported by the LMR promotes the depositional features in the LMV. All of the major

geomorphic features of the alluvial valleys such as meander belts, floodbasins, valley trains, alluvial aprons, terraces, lacustrine basins, and the deltaic plain are present in the LMV (Smith, 1996).

2.2.1.1 Meander Belts:

Abandoned and active meander belts are the most evident geomorphic features in the LMAV. A set of meandering belts form when a river has a low gradient, a high suspended load to bed load ratio, relatively steady annual discharge, a relatively constant base level and cohesive bank materials (Saucier, 1994). The Mississippi River met all these requirements during the Holocene when it was not conveyed by pulses of meltwater and glacial outwash (Saucier, 1994). All the meander belts are comprised of low natural levees, which are low ridges that slope gently away from the parent channel to the level of adjacent floodplain (Smith, 1996). In addition to natural levees, meander belts include crescent-shaped oxbow lakes, point bar ridge and swale topography, and occasional crevasses and crevasse channels along the outside bends of former channels and courses (Smith, 1996).

2.2.1.2 Floodbasins:

Floodbasins (backswamps) are broad and extremely flat areas between the higher meander belts and valley trains (Smith, 1996). Floodbasins are the lowest parts of the floodplain and consist of mostly gray to black clays and silty clays with thin laminations deposited by local accretion during floods (Farrell, 1987; Saucier, 1994). Backswamps of the LMAV are generally abundant in organic matter both as woody fragments and scattered small particles (Saucier, 1994). Drainage patterns in backswamps of LMAV are usually erratic, with small, often interconnecting channels (Smith, 1996).

2.2.1.3 Valley Trains:

Valley trains in the LMV were first recognized by Fisk (1944) who interpreted these features to be deposited from glacial outwash discharge into the LMV by the braided Mississippi, Ohio, and Arkansas rivers. The valley trains were referred to as braided stream terraces or braided relict alluvial fans and Autin et al. (1991) suggested that these features be called valley trains. Valley trains are most abundant in the upper third of the LMV and remained exposed in the middle third of the LMV (e.g., Macon Ridge) (Smith, 1996). Braided channels and interfluves between the channels are the main landforms of valley trains in the LMV (Smith, 1996). Autin et al. (1991) and Saucier (1994) suggested that these valley trains are variable in age in the LMV.

2.2.1.4 Alluvial aprons and the valley bluff:

Both alluvial fans and colluvial aprons occur at the base of the LMV bluff (Smith, 1996), which is a broad, rounded cliff that forms the boundary of the alluvial valley. Alluvial aprons exist at irregular intervals along all LMV bluff lines but are well developed where the bluff is eroded into Tertiary and older deposits (Smith, 1996). Alluvial fans are low, gently sloping masses of fluvial sediment that are deposited where a stream discharges from the upland into a low-lying plain. In the LMV, alluvial fans occur primarily between Baton Rouge and Cairo, along with both sides of Crowley's Ridge between Cape Girardeau and Helena and at the base of the Ozark escarpment north of the mouth of the White River (Saucier, 1994). The eastern bluffs along the LMV are covered with loess deposits, and underneath these deposits fluvial sand and gravel deposits have been identified (Smith, 1996). Colluvial aprons are also well developed along the steep eastern bluff line, and are formed by commonly small mass failures of the

loess-covered bluff line and occasionally large mass failures in the form of rotational slides.

2.2.1.5 Lacustrine basins:

Generally, lacustrine sediments that were deposited under low-energy conditions are characteristic with fine-grained, well-sorted deposits in shallow, freshwater lakes (Saucier, 1994). There are many contemporary and relict lacustrine basins within the LMV. Catahoula Lake in central Louisiana, Lake St. Francis and Big Lake in northeastern Arkansas, Reelfoot Lake in western Tennessee, and Lake Monroe of the Ouachita valley in south-central Arkansas are some of the largest lacustrine basins in the LMV (Smith, 1994). However, the Atchafalaya lacustrine basin in the deltaic plain is the largest in the LMV (Smith, 1994).

2.3 INFLUENCE OF QUATERNARY GLACIATIONS AND HUMAN MODIFICATIONS

2.3.1 Influence of Quaternary Glaciations.

Even though the LMR is located in a relatively stable tectonic position, the headwaters of the Upper Mississippi River have been subject to considerable modification during the last 2.5-3.0 million years in response to regional advances and retreats of continental glaciers (Knox, 2007). A little more than 75% of the drainage basin of the Mississippi River occurs upstream of the head of the LMAV at Cairo, IllinoisMoody and Meade (1993) showed that 84% of the mean annual discharge and 88% of the mean annual sediment load delivered to the LMAV comes from the Missouri, upper Mississippi, and the Ohio tributary systems. Therefore, fluvial activity in the LMAV is strongly influenced by the Great Plains and upper Mississippi valley drainage

system. Continental glaciation is the most significant geologic process responsible for geomorphic changes in the LMAV.

LMAV valley was influenced by mainly four episodes of environmental changes from Late Quaternary to present. Distinctive changes to the LMV began with a long period of progressive valley aggradation starting from 25,000 to 14,000 years B.P. During this period meltwater from the Upper Mississippi Valley transported large quantities of sediment into the LMV (Knox, 1996). Late Wisconsin to Holocene transition period during 14,000 to 9,000 years B.P., resulted in the second episode of environmental changes because of large catastrophic floods associated with rapid drainage of proglacial lakes (Knox, 1996). The third episode during the Holocene period began at about 9,000 years B.P. and concluded between 150–200 years ago. Finally, the most recent noteworthy changes to the LMV represent a period strongly influenced by human activities such as constructing dams, artificial levees, and other structures along the LMV (Knox, 1996).

During the late Wisconsin age (25,000–14,000 years B.P.) almost the entire region of Canada, and the some regions of New England, the Midwestern United States north of the Ohio and Missouri rivers, Idaho, Montana, and Washington were covered with regional ice sheets (Knox, 2007). The Mississippi River system drained nearly the entire southern margin of the continental ice sheet during the Wisconsin age of glaciation (Knox, 2007). Meltwater pulses transported massive quantities of sand- and gravel-sized sediment downstream. As a result of the huge sediment supply, aggradation of sand and gravel occurred seaward to the continental shelf and the Mississippi fan sedimentation cone in the Gulf of Mexico (Autin et al., 1991). The LMV during the late Wisconsin was

a wide braided river along the western side of the current LMV in southeastern Missouri and eastern Arkansas (Autin et al., 1991; Saucier, 1994).

Advancement of glaciers resulted in maximum ice sheets spreading at about 18,000 years B.P. followed by a gradual retreat northward (Knox, 2007). By 14,000 years B.P., the general northward retreat of ice sheets resulted in large proglacial lakes between the continental glacier and former ice front positions. The next episode of environmental changes in the LMV between 14,000 and 9,000 years B.P. was mainly because of large floods from these proglacial lakes. Proglacial lakes trapped most of the meltwater associated sand- and gravel- sized sediments while runoff from the lakes transported a diminished, but constant, supply of sediment to the LMV (Teller, 1987). Furthermore, outlets of many proglacial lakes failed catastrophically resulting in substantial erosion along the downstream river system (Teller, 1987). Avulsions created by these large catastrophic floods shifted the LMR position from the western lowlands to its present day position along the eastern margin of the valley (Blum et al., 2000). A shift from the late Wisconsin braided morphology to a meandering system concomitant with valley aggradation of fine grained sediments began near the mouth about 12,000 years B.P. and reached the head of the LMV near Cairo, Illinois, by about 9,000 years B.P. (Autin et al., 1991; Saucier, 1994). Tens of meters of late Wisconsin sediment deposits were removed by the Mississippi River during the pattern shift, which were replaced with inset point-bar and natural levee alluvium consisting mostly of clay and silt (Autin et al., 1991; Knox, 2007). Overbank flooding resulted in backswamp deposition and thickness of backswamps deposits increased downstream.

The transition from the late Wisconsin to the Holocene was characterized by global warming, which resulted in most of the environmental changes within the LMAV during the Holocene. According to Milliken et al. (2008), during the early Holocene between 10,000 to 8,000 years B.P. sea level was rising at a rate about 4.2 mm per year along the northern Gulf of Mexico shoreline. The rate of sea level rise during the middle Holocene period between 8,000 to 4,000 years B.P. was 1.4 mm per year (Milliken et al., 2008). The sea-level rise during both early and middle Holocene inundated the lowermost Mississippi River valley and set the stage for deltaic lobe development in southern Louisiana (Frazier, 1967).

During the Holocene, most of the Missouri River tributaries and upper reaches of Mississippi River tributaries draining the southern Great Plains were dominated by prairie grasslands (Knox, 2007). However, the Upper Mississippi River in Wisconsin and east-central Minnesota, the LMV, and the Ohio River drainage basin were dominated by forest vegetation cover (Knox, 2007). Grassland expansion eastward from the Great Plains occurred with maximum dryness between about 8,000 and 5,000 years B.P. near the Mississippi headwaters in north-central Minnesota (Dean, 1997; Knox, 2007). Farther to the southeast, in northeastern Iowa and southern Wisconsin, maximum dryness during the Holocene occurred between about 5,000 and 3,000 years B.P. (Knox, 2007). In the southern Wisconsin-northeastern Iowa region during the late middle Holocene warming of about 1.5℃ above the preceding period and reduction in the mean annual precipitation by about 15% less than today occurred.

Large overbank floods on the Upper Mississippi River during the Holocene were dominated by snowmelt runoff exacerbated by spring and summer rainfalls (Knox, 2007).

Floods on the Upper Mississippi River with 1-2 year recurrence intervals occurred as a result of either spring snowmelt or excessive summer rainstorms (Knox, 2007). A dramatic increase in short-term variability involving frequent fluctuations between moderately large floods and extremely small floods is characteristic of flooding along the Upper Mississippi River during the Holocene (Knox, 2007). However, flood records show an abrupt shift to larger floods after about 3,100 years B.P., which is consistent with a return to a somewhat cooler and moister climate (Baker et al., 1998; Knox, 2007).

2.3.2 Human modifications to the sediment regime of the LMV and modern floodplain.

No significant changes occurred to the LMAV during late Holocene to the beginning of the 20th century. With the beginning of the 20th century, significant environmental changes to the LMAV were introduced largely because of the human activities. As a result of more human settlement in the LMAV and growing agricultural practices, frequent flooding from the LMR became more hazardous for people and the croplands. The growing river commerce, together with increasing destruction caused by floods, was creating demand in navigation improvements and flood protection.

The Mississippi River is one of the most heavily regulated rivers in the world and most modifications to the river were introduced after 1929 (Kesel, 2003). Fifteen meander bends were cut-off and isolated to channelize the LMR in order to improve and maintain navigation between the years 1929 and 1942 (Kesel, 2003). As a result, the LMR was shortened by 245 km. The LMR was shortened again by 88 km between 1939 and 1955 by chute cut-offs (Kesel, 2003). There are nine dams and two lock and dam structures between Lake Itasca, the headwaters of the Mississippi River, and

Minneapolis, Minnesota (Horowitz, 2010). Additionally, twenty-six lock and dam structures were built from 1917 to 1953 between Minneapolis and downstream of St. Louis, Missouri (Horowitz, 2010).

After the 1927 flooding event, 3,000 km of artificial levees were either constructed or raised downstream of St. Louis, which separated the floodplain from the river channel and resulted in reducing overbank inundation by 90% (Kesel, 2003). After 1940, 1,400 km of concrete revetments were introduced along the channel and, consequently, reduced bank caving and eliminated lateral migration of the channel (Kesel, 2003). Since 1955, dikes have been constructed to trap bed sediments.

Prior to these modifications along the Mississippi River an estimate of about 270 * 106 m3/year of the suspended load, and 130 * 106 m3/year of bedload sediment were transported to the Gulf of Mexico (Kesel et al., 1992). The LMAV sediment regime served as both a sediment source and as a short- and long-term storage location. Nearly two-thirds of bed load sediments transported by the river from Cairo to Red River Landing was generated as result of bank caving as the river meandered through the floodplain (Kesel et al., 1992). This river segment also stored sediment within the channel in the form of river bars and as floodplain deposits (Kesel et al., 1992). The river segment between Red River Landing and the Gulf of Mexico served as a conduit to transport sediment. Less sediment was added from bank caving or by tributaries to the LMAV and most of the sediment stored in this segment was from overbank floodplain deposition (Kesel et al., 1992).

After the construction of most of the engineering structures along the Mississippi River, there was a major net sediment decrease from both tributaries and floodplain

sources (Kesel, 2003; Horowitz, 2010). Meade and Moody (2010) showed that structures introduced to the Missouri and Arkansas rivers accounted for 50% to 70% of the reduction of suspended sediment reaching the Gulf of Mexico. Additionally, Horowitz (2010) recognized a sharp decrease in the long-term rate of suspended sediment concentrations associated with the flooding event of 1993. Horowitz (2010) further concluded that long-term reduction in sediment supply to the Gulf of Mexico results from numerous engineered structures along the river and the 1993 flooding event resulted in flushing massive quantities of stored, readily erodible sediments from the basin.

2.4 SOIL NUTRIENTS

In addition to the river shortening and engineering structures built after 1929, agricultural practices within the Mississippi basin also changed at about the same time. Since 1950, there was a significant increase in use of chemical fertilizer and consequently increased runoff of nutrients, such as, nitrogen (N) and phosphorus (P) downstream and ultimately deposited in the Gulf of Mexico (Donner and Kucharik, 2003; Schönbrunner et al., 2012).

Nutrients were introduced to the LMAV soils through the overbank sedimentation during the natural flooding. Floodplain soil can be both a source and a sink for N and P as it provides a medium for many biological, chemical, and physical reactions (Brady and Weil, 2008).

2.4.1 Nitrogen (N)

The distribution of N in soil profiles closely parallels that of soil organic matter as most of the N on land is found in soil bound organic matter. Exceptions can occur where large amounts of fertilizer have been applied; inorganic N rarely accounts for more than 1 to 2% of N in the soil (Brady and Weil, 2008). Nitrogen is available to plants as either ammonium (NH_4^+) or nitrate (NO_3^-) and these two are critical forms of inorganic N in the N cycle. In addition to the possible loss to erosion and runoff, both of these ions can be subject to loss from the soil by immobilization by microorganisms and removal by plant uptake. Volatilization is another process which can reduce the N content in the soil. Ammonium can be fixed in the interlayer of certain 2:1 clay minerals; further, it can be oxidized to nitrite and subsequently to nitrate by a microbial process called nitrification (Khalil et al., 2004). Similarly, nitrate can be lost to groundwater by leaching in drainage water and also can be reduced to ammonium form by anaerobic organisms (Brady and Weil, 2008). In flooded soils, denitrification is more prominent which reduces nitrate to such gasses as NO, N_2O, and N_2, a process of volatilization. In the Lower Mississippi alluvial plain where soils are subject to alternate periods of wetting and drying, nitrates that are produced by nitrification during dry periods are subject to denitrification when the soils are submerged (Mitsch et al., 2001). As floodwaters move on to the floodplain and the soil becomes anaerobic, perfect conditions are produced for microorganisms to reduce nitrate to gaseous forms (Schramm, 2009).

2.4.2 Phosphorus (P)

Phosphorus is classified as a macronutrient because of the large amounts of P required by plants to synthesize. Compared to other macronutrients such as nitrogen and

sulfur, the concentration of P in soil solution is very low, generally ranging from 0.001 mg/L in very infertile soil to 1 mg/L in well-fertilized soils (Brady and Weil, 2008). Plant roots absorb phosphorus dissolved in the soil solution as phosphate ions (PO_4^{3-}). Mainly there are three general groups of the compound: (i) organic phosphorus, (ii) calcium-bound inorganic phosphorus, and (iii) iron- or aluminum-bound phosphorus in which the bulk of soil P exists (Brady and Weil, 2008). In addition to surface runoff and erosion, principal ways of removing P from the soil system is plant removal and leaching to groundwater. Under well-aerated soils availability of P is generally low because most of the P compounds are insoluble (Schönbrunner et al., 2012). However, prolonged anaerobic conditions in LMAV make iron-phosphate complexes much more soluble and cause the release of P into solution (Schramm, 2009; Schönbrunner et al., 2012). In contrast to N, P tends to increase in concentration during the flooding season compared to dry seasons.

In this study, sediment layers with high and low nutrient levels within the core samples are expected to correlate with flooding and drying seasons, respectively. Upstream structures built to facilitate commercial navigation and to reduce flooding of agricultural lands and communities are responsible for altering the nutrient concentration levels sequestered in the soil system (Schramm, 2009) Because of those structural changes, the Lower Mississippi River floodplain is receiving higher water levels of shorter duration (Wasklewicz et al., 2004). Also, the water temperatures have become colder and area of floodplain inundation has become smaller. According to Schramm (2009), 542 kg N ha^{-1} can be removed or sequestered in the Lower Mississippi River

floodplain during the present hydrologic conditions for two months whereas historical conditions sequestered 976 kg N ha^{-1} for a three month inundation period.

2.4.3 Soil Organic Matter and Carbon (C)

Plants can absorb atmospheric carbon dioxide through the process of photosynthesis, whereby the energy of sunlight is trapped as chemical energy in the form of carbohydrate molecules. Some organic materials are stored temporally as constituents of standing vegetation despite some of this organic matter being used as source of energy by plants themselves (Brady and Weil, 2008). Organic carbon can enter to the soil through plant and animal residues or root deposition. Soil organic carbon can be lost as carbon dioxide from the soil through metabolic processes of soil organisms (Sahrawat, 2003; Brady and Weil, 2008).

Carbon can be present in both organic and inorganic forms in soil. Weathering of C-bearing minerals or reactions of soil minerals with atmospheric carbon dioxide can result in the mineral form of soil inorganic C. In the LMAV, the dominant form of C in the soil is organic C. Soil organic C includes both dead and living soil biotic materials. Plant residue decomposition, which is the breakdown of large organic molecules into smaller components, is the primary source of soil organic matter (Sahrawat, 2003; Brady and Weil, 2008).

In aerobic soils, three primary microbiological reactions occur that decompose organic matter: (i) enzymatic oxidation of carbon compounds, which breaks down long chain polymers such as cellulose and starch into short chains; (ii) release and/or immobilization of nutrient elements such as nitrogen, phosphorus, and sulfur; and (iii) creation of resistant compounds through modification of the original compound (Brady

and Weil, 2008). However, in anaerobic conditions decomposition takes place very slowly in comparison to aerobic conditions, hence accumulation of substantial amounts of soil organic matter (Sahrawat, 2003; Six et al., 1998). Table 2.1 summarizes nutrients concentrations recorded for sediments from different environments from different studies.

Table 2.1

N, C, and P concentration values from different environments.

Environmental type	**N (%)**	**C (%)**	**P (µg/g)**
Depressional Marsh (a)	0.22 ± 0.05	2.5 ± 0.7	31 ± 7
Depressional Savanna (a)	0.2 ± 0.06	2.6 ± 0.9	116 ± 46
Depressional Forest (a)	0.72 ± 0.09	10 ± 1.3	717 ± 92
Forested Floodplain (a)	0.38 ± 0.08	5.2 ± 1.3	335 ± 68
Floodplain (b)	0.18 ± 0.03	2.35 ± 0.48	240 ± 25
Levee (b)	0.16 ± 0.02	1.83 ± 0.27	370 ± 22

All the concentrations values are for the top 0-30 cm of soil

(a) - floodplain wetlands of southwestern Georgia, USA (Craft and Casey, 2000)

(b) - floodplain wetlands of the Altamaha River, Georgia, USA (Bannister et al., 2016)

2.5 MAGNETIC SUSCEPTIBILITY (MS) OF SOIL

Fluvial sediments are composed of both detrital and biogenic components. There are also components derived from sediment weathering processes, but these are generally minor (Johnsson and Meade, 1990). All mineral grains are susceptible to magnetism in the presence of a magnetic field, and magnetic susceptibility (MS) is the measure of the strength of the transient magnetism within the sample (Ellwood et al., 2006; Dearing, 1994). Ferrimagnetic minerals such as the iron oxides magnetite and maghemite, and iron sulfide and sulfate minerals, including pyrrhotite, can acquire remanent magnetism. Magnetizable materials also include paramagnetic compounds such as iron-rich clays, particularly chlorite, smectite, and illite; ferromagnesian silicates such as biotite, pyroxene, and amphibole; and other iron and magnesium bearing minerals (Ellwood et

al., 2000). The presence of ferromagnetic and paramagnetic compounds will increase the MS values in a sediment sample. In addition to ferrimagnetic and paramagnetic grains in sediments, the presence of abundant minerals like calcite and/or quartz, as well as organic compounds, can lower the MS values (e.g., Heitmuller and Hudson, 2009). These diamagnetic compounds typically acquire a negative MS when placed in an inducing magnetic field. Low-field MS is parameterized as *k*, indicating that the measurement is relative to a 1 m^3 volume and therefore is dimensionless. Mass specific susceptibility (m^3 kg^{-1}) can be taken by dividing the *k* value by the bulk density of the sediment sample. Table 2.2 summarizes some of the typical magnetic susceptibility values range of various materials.

Table 2.2

Typical ranges of room temperature magnetic susceptibility values measured for environmental materials and minerals.

Environmental materials and minerals	**MS values (* 10^{-6} m^3 kg^{-1})**
Ferrimagnetic minerals	> 30
Burned soils	0.2 - 90
Basic/ultra basic rocks	9 - 30
Top soils	0.01 - 15
Felsic Igneous rocks	0.02 - 8
Paramagnetic minerals	0.01 - 3
sedimentary rocks	0.001 - 0.1
Diamagnetic minerals	< -0.001

(From Dearing, 1994).

CHAPTER III – STUDY AREA

3.1 GENERAL DESCRIPTION OF THE STUDY AREAS

The study area is located in the St. Catherine Creek and Cat Island National Wildlife Refuge (NWR) complex along the Lower Mississippi River (LMR) in southwestern Mississippi and southeastern Louisiana (Figure 3.1). St. Catherine Creek NWR is located south of Natchez in western Adams County, Mississippi. The western boundary of the refuge is the Mississippi River and the eastern boundary follows the bluff line. The bluff line is a series of seperated loess capped low-lying hills which are underlain by the Citronelle Formation and Hattiesburg Formation. The southern boundary of St Catherine Creek is the Homochitto River. St. Catherine Creek NWR includes over 24,000 acres and all sample locations receive flood waters and sediment from the Mississippi River from winter through early summer. Moist-soil impoundments, reforested areas, fallow fields, and accreted meander scrolls occur in this area. Cat Island NWR is located near St. Francisville, Louisiana, which is 30 miles north of Baton Rouge. The assemblage of landforms, land-use conditions, and flood characteristics at Cat Island NWR is similar to those at St. Catherine Creek NWR.

St. Catherine Creek and Cat Island NWR are managed as a part of the LMR refuge complex along with Bayou Cocodrie NWR. The primary management objective of the refuge complex is to maintain the integrity of a dynamic bottomland hardwood forest ecosystem in the LMR valley (U.S Fish and Wildlife Service, 2014). In the late 1960's, two thirds of the present-day St. Catherine Creek NWR was cleared for row-crop agriculture. Since the establishment of the refuge complex in 1990, much of the land has been planted back to original, native bottomland hardwood tree species. About 30% of

the St. Catherine Creek NWR land area consists of bald cypress swamps and hardwood forests teeming with oak, gum, elm, ash, and cottonwood. Nearly 10% of the acreage is open water and the remaining area consists of cleared land and land created from channel migration of the Mississippi River. Cat Island NWR was established in 2000 to conserve, restore, and manage native forested wetland habitats (U.S Fish and Wildlife Service, 2014). Cat Island NWR also consists of bottomland hardwood forests composed of oak, elm, and hickory and nearly 3,000 acres of cypress-tupelo swamp habitat.

The present-day LMR has been artificially leveed along the majority of its length (Smith and Winkley, 1996; Knox, 2007). This, in combination with river dredging and straightening, has reduced the floodplain to a narrow stretch to protect farmlands and cities. The study areas can be considered as the one of few areas within the LMR alluvial valley that exist without artificial levees on their side of the river channel and, thus, flood naturally. Because of the high connectivity of the LMR with the floodplains, St. Catherine Creek and Cat Island NWRs are greatly influenced by annual inundations of floodwater from the Mississippi River. The annual floodwater creates a recurring wet and dry season along the floodplain. During summer and fall plants grow quickly because of the dry season and during spring and winter most of the land area is inundated. The annual floods deposit a rich nutrient layer to support this highly dynamic system rich in biological diversity and abundance.

Five soil cores were collected from St. Catherine Creek NWR, two cores were collected from Cat Island NWR, and one core was collected on private property adjacent to Cat Island NWR in October 2015 during relatively dry conditions when the floodplain was most accessible. Table 3.1 summarizes the eight sample locations.

Table 3.1

Core sample locations and characteristics in St. Catherine Creek (SC) and Cat Island (CAT) National Wildlife Refuges.

Core Sample	Latitude (N)	Longitude (W)	Elevation (m)[1]	Distance to main River (km)[1]	Sub-Environment[2]
MS.SC 01	31˚20' 05.97"	91˚29' 02.08"	15.25	1.45	Backswamp
MS.SC 02	31˚20' 57.19"	91˚28' 01.20"	15.25	1.27	Backswamp
MS.SC 03	31˚21' 06.97"	91˚26' 37.47"	16.46	2.8	Backswamp
MS.SC 04	31 ˚21' 16.32"	91˚27' 44.70"	16.76	1.21	Backswamp
MS.CAT 05	30 ˚47' 13.63"	91˚27' 18.27"	9.75	4.8	Backswamp
MS.CAT 06	30 ˚45' 39.50"	91˚29' 48.49"	10.36	1.4	Point bar
MS.CAT 07	30 ˚47' 57.19"	91˚31' 14.23"	14.33	0.8	Levee backslope
MS.SC 08	31 ˚28' 04.54"	91˚28' 36.03"	14.33	3.21	Point bar (swale)

[1]Elevation and distance values derived from Google Earth.

[2]Sub-environments from Saucier (1994).

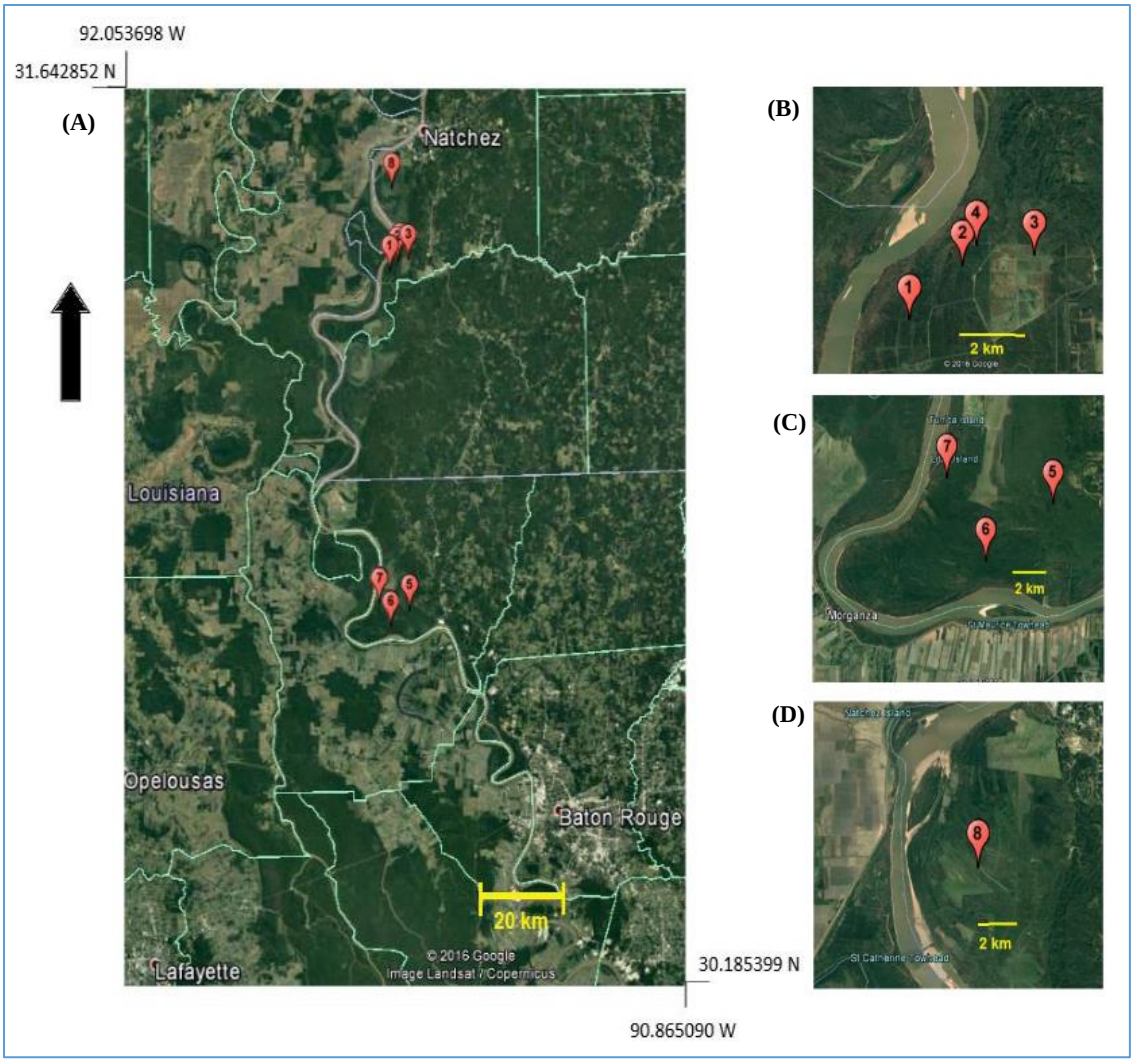

Figure 3.1 Sample core locations.

(A) Sample core location of MS.SC 01 in St. Catherine Creek NWR. (B) Sample core location of MS.SC 03 in St. Catherine Creek NWR. (C) Sample core location of MS.CAT 05 in Cat Island NWR. (D) Sample core location of MS.SC 08 in St. Catherine Creek NWR.

3.2 DESCRIPTION OF THE SAMPLE LOCATIONS

3.2.1 MS.SC 01: Backswamp

Soil core sample location MS.SC 01 is located in the Sibley unit in St. Catherine Creek NWR. The location was accessed by motor vehicle along Pintail Lane and a ~500

m walk along an ATV trail. The sample location is about 30 meters north of the ATV trail. There are two ATV trails to the west in between sample site and the river at about 250 m and 750 m from the sample site that can influence the natural overbank sedimentation during floods.Sample location is surrounded by 30 to 40-year wooded growth, including willow trees shown in Figure 3.2A. The core samples were extracted from a cleared area between sycamore trees. The sample core is from a minor topographic floodplain relief within the backswamp.

3.2.2 MS.SC 02: Backswamp

MS.SC 02 is located in the Sibley unit in St. Catherine Creek NWR. The sample location was accessed by motor vehicle along Pintail Lane and a ~500 m walk along an ATV trail. The sample location is about 25 meters south of the ATV trail. Artificial ATV trail that is about 500 m to the west of the sample location can influence the natural overbank sedimentation during floods. The location of MS.SC02 is surrounded by relatively tall willow trees and the ground area is covered with shrubs.

3.2.3 MS.SC 03: Backswamp

The MS.SC 03 sample core was collected from a swamp area of the Sibley unit in St. Catherine Creek NWR and was accessed by a motor vehicle along Pintail Lane and a subsequent wade across a mud-filled ditch. Ditch is about 125 m northeast of the sample location. Sample location represents a minor topographic depression within the backswamp deposit. The sample location occurs in a large cleared field shown in the Figure 3.2B. The groundwater table here was detected at a depth of ~100 cm and a number of fibrous woody tissues also were recovered from the soil core at ~115 cm.

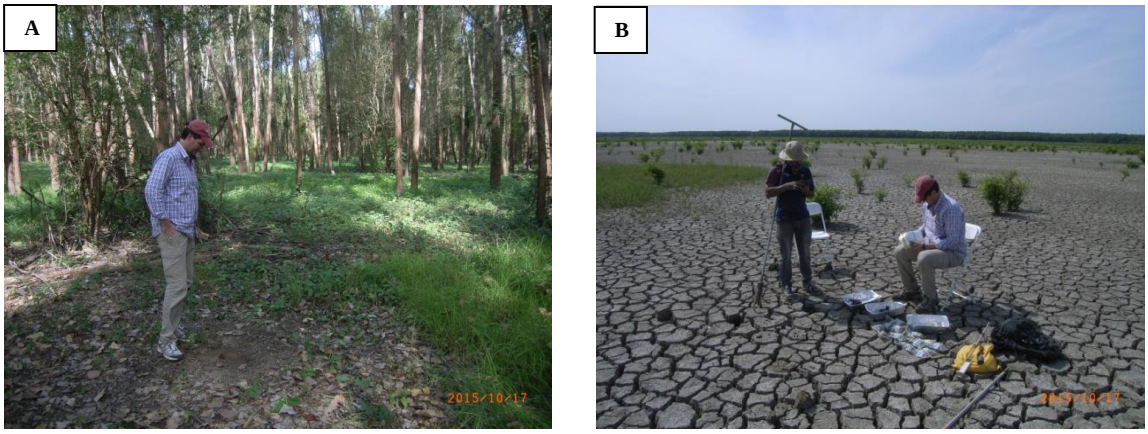

Figure 3.2 Sample core locations.

(A) Sample core location of MS.SC 01 in St. Catherine Creek NWR.

(B) Sample core location of MS.SC 03 in St. Catherine Creek NWR.

3.2.4 MS.SC 04: Backswamp

MS.SC 04 is another backswamp deposit located in the Sibley unit in St. Catherine Creek NWR. The sample location was accessed along an ATV trail starting at the far north end of Pintail Lane. Sample location is about 30 m south of the ATV trail and ATV trail can affect the natural overbank sedimentation during floods. The surrounding area is covered with willow trees.

3.2.5 MS.CAT 05: Backswamp

MS.CAT 05 is located in a backswamp in Cat Island NWR. The sample site was accessed along an ATV path of the Blackfork Trail. The ATV trail is about 50 m south of the sample location. The sample site was surrounded by bald cypress trees (Figure 3.3A). The sample site located in relatively low topographic level and fresh evidence of 2015 flood inundation earlier in the year (2015) was observed as well-preserved seed lines

representing recessional phases. The highest seed line observed in the area was about 3.2 meters above the floodplain surface.

3.2.6 MS.CAT 06: Point-Bar

MS.CAT 06 occurs in a meander scroll (i.e., point-bar deposit) setting at Cat Island NWR. The vegetation is dominated by bald cypress trees, much similar to that of MS.CAT 05 location (Figure 3.3A). The sample location was accessed along an ATV trail that was bordered by a ~1.5 meter high berm oriented parallel to the trail. The sample location is about 50 meters south of the ATV trail and berm and this ATV trail can influence on natural overbank sedimentation during flooding. The sample location situated in a relatively minor topographical depression.

3.2.7 MS.CAT 07: Levee Backslope

MS.CAT 07 is along a natural levee backslope located at a privately-owned property in the vicinity of Cat Island NWR. The sample location is on a small topographical relief. The sample location is about 50 meters west of Cat Island Road. An artificially-modified drainage occurs along the west side of the road. The area is covered with willow trees; a clear silt line that might be related to the 2015 flood was observed on a furrowed tree trunk ~35 cm above the ground surface.

3.2.8 MS.SC 08: Point-Bar

MS.SC 08 is located in the Cloverdale unit of the northern part of St. Catherine Creek NWR. The sample core was collected from a swale deposit where well developed ridge-and-swale topography is present. No trees were present at the sample site but small deciduous plants covered the ground surface (Figure 3.3B). In between the sample location and the river, Carthage Point road runs parallel to the river and located about 2

km west of the road. However, there is a small road in the vicinity of the sample location at about 175 m to the south of sample site.

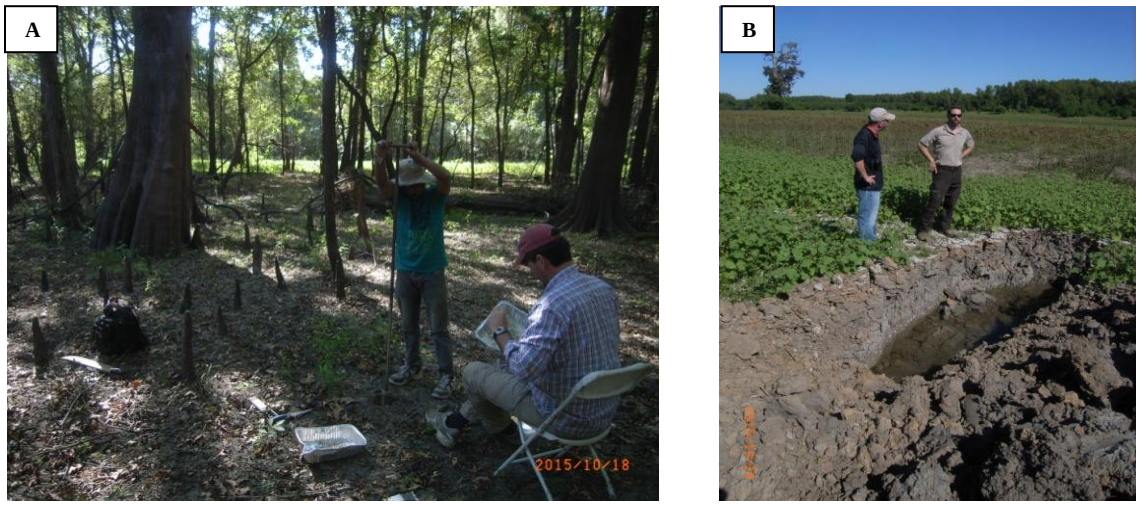

Figure 3.3 Sample core locations

(A) Sample core location of MS.CAT 05 in Cat Island NWR.

(B) Sample core location of MS.SC 08 in St. Catherine Creek NWR.

CHAPTER IV – METHODOLOGY

4.1 PRELIMINARY INVESTIGATION

Before departure to the field, a preliminary investigation was accomplished based on available information from published geological literature of the study area. Available geological maps, topographic maps, Google Earth images, and other information about the area were reviewed prior to the field visit in order to discern topographic details, location accessibility, and other pertinent information.

4.2 SAMPLE COLLECTION

Eight sample sites were selected from the Lower Mississippi alluvial floodplain (Figure 3.1), which represent different depositional sub-environments including natural levees, point bar ridges and swales, and backswamps. Sample core MS.SC01 was sampled at 10-cm increments to a depth of 170 cm. Sample core MS.SC02 was sampled to a depth of 250 cm and samples were collected at 5-cm increments. The remaining six sediment cores were sampled at 5-cm increments to a depth of 150 cm below the surface. A soil auger was used with an extension to obtain the sediment cores (Figure 4.1). A 2-m folding rule was used to ensure accurate depth increments. Sediment samples from each depth increment were placed in sample bags and immediately transferred to a cooler with ice packs to maintain a low temperature before transfer into a refrigerator for storage in order to minimize microbial degradation of nutrients. GPS coordinates of the eight samples sites were noted and, if discernible, sedimentation thickness of the uppermost soil lamination was recorded, which represents sediments deposited by the most recent flooding event during summer 2015.

Figure 4.1 Collecting and lebeling sediment samples.

(A) Using a soil auger to get the sediment sample at MS.SC01 in St Catherine Creek NWR, (B) Placing sediments in sample bags and labeling the sample bags at MS.SC02 in St Catherine Creek NWR

4.3 LABORATORY ANALYSIS

The sediment samples were analyzed for organic matter content (%), magnetic susceptibility (X), and particle size (mm) in the USM Sedimentology Laboratory. Carbon (C), nitrogen (N), and phosphorus (P) content at each depth increment were measured using equipment and supplies from the USM Department of Biological Sciences.

Part of sediment samples were oven dried at 105°C overnight. Subsequently, the dried soil samples were physically disaggregated using a mortar and pestle as preparation for analyzing organic content, magnetic susceptibility, and particle size.

4.3.1 Organic content

Approximately 2 g of dry soil was measured using an electronic scale and the initial weight of the sample was recorded. The weighed sample was placed in a ceramic crucible (with a lid) and combusted in a muffle furnace for four hours at 550°C. The final mass of the sediment sample was recorded after cooling to room temperature. Organic content (%) of all soil samples at each depth increment was computed as the percent weight loss by ignition.

4.3.2 Magnetic susceptibility

Magnetic susceptibility (MS) (SI) was measured for all soil samples at each depth increment using a Bartington MS3 magnetic susceptibility instrument and MS3 Bartsoft software (version 2.3.1.1). Oven-dried soil was transferred into vials designed for the magnetic susceptibility meter and MS values at both low frequency (0.46 kHz) and high frequency (46 kHz) were recorded. Sample volume was kept constant at 10 cm^3 for all the samples. For subsequent data analysis, low frequency values were used because according to Dearing (1994), sediments smaller than 0.03 μm show reduced MS values at high frequency.

4.3.3 Particle Size analysis

Particle size was analyzed for all depth-increment samples from each sediment core according to procedures outlined in Gee and Bauder (1986). Hydrogen peroxide (30% H_2O_2) was added to the oven-dried soil samples to remove all remaining organic matter and samples were subsequently re-dried. For each dried, organic-free sample, 50 g of sample was used to analyze particle size. For chemical disaggregation of clays, 250 ml of distilled water and 100 ml of 5% sodium hexametaphosphate solution were added to

each soil sample. The mixture was kept overnight and during the following day the sample mixture was further physically disaggregated for 7 minutes using a milk-shake mixer. The sediment mixture was poured into a Bouyoucos tube and distilled water was added up to the 1000 ml line. In an another Bouyoucos tube, a 'control' was prepared using 100 ml of 5% hexametaphosphate solution and 900 ml of distilled water. A rubber stopper was placed on the Bouyoucos tube with the sediment mixture, which was shaken for 1 minute. After the tube was placed on the counter, a stopwatch was immediately started. A 152-H hydrometer was gently placed into the Bouyoucos tube and specific gravity values at various time increments were recorded. Alongside the sediment mixture, fluid temperature and specific gravity values were recorded in the control tube using the same hydrometer. After three days of settling and recording specific gravity values, the sample mixture was poured into a stack of USA standard phi -1 (X mm), 0 (X mm), 1 (X mm), 2 (X mm), 3 (X mm), and 4 (X mm) sieves. Next, sediment was washed out of each sieve into pre-weighed and labeled 150 ml beakers. Finally, beakers were oven dried at 105℃ for 24 hours and the dry weight of each beaker with sediment was measured using a digital scale. Particle-size distribution graphs were rendered and clay, silt, and sand percentages for each soil sample were calculated in a pre-formatted Microsoft Excel spreadsheet according to principles of Stokes' Law that account for temperature-based variations in fluid density and viscosity during the 3-day analysis.

4.3.4 Nutrient analysis

Depth-increment sediment samples were stored in a freezer to convert all moisture into ice. A lyophilizer was used to dry the ice and this procedure was repeated until moisture was completely removed. The dried sediment sample was crushed using a

mortar and pestal and passed through a 250-micrometer sieve. Three 20-mg sediment samples for each 5-cm depth increment were subsequently prepared to measure C and N. For the P analysis, 100 mg of the sediment sample was used.

4.3.4.1 C and N analysis

C and N analyses were done using a Costech elemental combustion system. Before analysis, two conditioning samples (sediment) were tested at the beginning of each round to ensure the instrument was operating correctly. Four standards of Attropine (weights 0.250 mg, 0.5 mg, 0.75 mg, and 1.0 mg) were analyzed immediately after the conditioning samples to calibrate the instrument before the sediment samples were analyzed. For quality control purposes, 3 mg of Base Culm was analyzed in the instrument after every 10 samples. Sample cores MS.SC01 and MS.SC08 were analyzed at each depth increment to depths below surface of 170 cm and 145 cm, respectively. The remaining six cores were analyzed at each 5-cm increment to a depth below surface of 125 cm.

4.3.4.2 P analysis

For P analysis, 100 mg of the sediment sample was combusted in a muffle furnace at 550 °C for four hours. After that, a hot HCl acid extraction was prepared by warming 10 ml of 1 mol/l HCl acid in a hot water bath at 85°C for 30 minutes. To dilute the acid, 10 ml of distilled water was added. A centrifuge tube with the sediment sample was mixed properly using a vortex mixer. Next, 0.1 ml of the diluted acid extraction and 10 ml of distilled water were added to the centrifuge tube, which was centrifuged for 10 minutes. Subsequently, the centrifuged sample was analyzed for P using SEAL AA3

Flow Injection Nutrient Analyzer equipment. Weight percentage values were calculated based on the P reading and the initial sample weight.

CHAPTER V – RESULTS

5.1 MS.SC01

Figure 5.1 is a graphical depiction of results for the MS.SC01 sediment core, which was collected in a backswamp environment in St. Catherine Creek NWR, Mississippi. Sediments of MS.SC01 are dominated by silt and clay particles, but there is about 20% sand in the topmost 50 cm below the surface. Below that, sediments consist of silt and clay size particles with proportionally more silt. Nitrogen and carbon weight percentages follow a similar pattern to each other. The highest percentages of N and C occur at the surface with values of 0.31% and 3.84%, respectively. Between 0 cm and 30 cm both N and C weight percentages decrease, and from 30 cm to 160 cm N and C have relatively constant values of 0.07% and 0.85%, respectively. The lowest values for N (0.04%) and C (0.6%) occur at 80 cm depth from the surface. Magnetic susceptibility (MS) values range from 242 * 10^{-6} to 589 * 10^{-6}. The highest value of 589 * 10^{-6} occurs at 50 cm depth and the lowest value of 242 * 10^{-6} occurs at 100 cm depth. Soil organic matter (OM) percentage values range from 5–10%. The highest value of 9.7% occurs at the surface and the lowest value of 5.3% occurs at 50 cm depth.

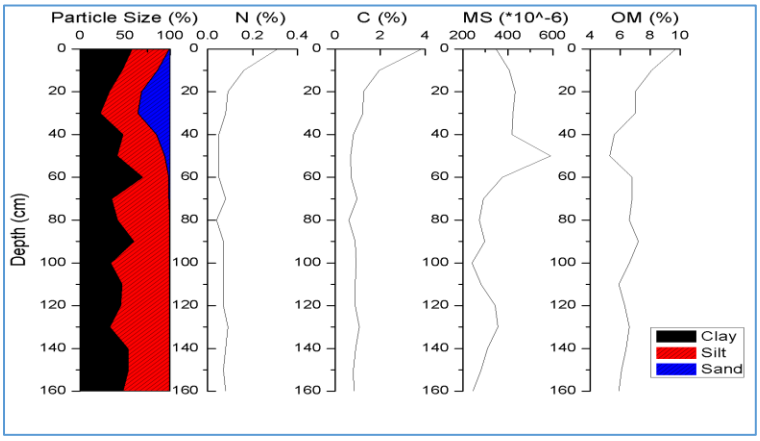

Figure 5.1 Particle size, N, C, MS, and OM results for sample site MS.SC01.

5.2 MS.SC02

Figure 5.2 is a graphical depiction of results for the MS.SC02 sediment core, which was collected in a backswamp environment in St. Catherine Creek NWR, Mississippi. MS.SC02 mainly consists of silt and clay particles, and the clay fraction gradually increases with depth from the surface. N and C percentages follow a relatively similar pattern with depth to each other. Both N (0.22%) and C concentrations (2.47%) have maximum values at the surface, and concentrations decrease to 0.09% and 1.05%, respectively, at about 25 cm depth. Between 25 and 80 cm both N and C values have relatively constant values of 0.09% and 1.14%, respectively, and from 85–120 cm N and C concentrations decrease again to an average value of 0.08% to 0.89%, respectively. The lowest MS value of 85 * 10^{-6} occurs at a depth of 195 cm below the surface and the highest recorded value is 472 * 10^{-6} at a depth of 55 cm. The highest OM percentage of 12.6% occurs at the surface and it decreases to 5.5% at about 30 cm depth. From 30–70 cm, the lowest OM values average 5.3%. From 75–185 cm depth, the average OM value is 6.5% and increase to an average of 9.0% between 190 and 215 cm. Between 215 and 245 cm the OM values again decrease to an average of 6.9%.

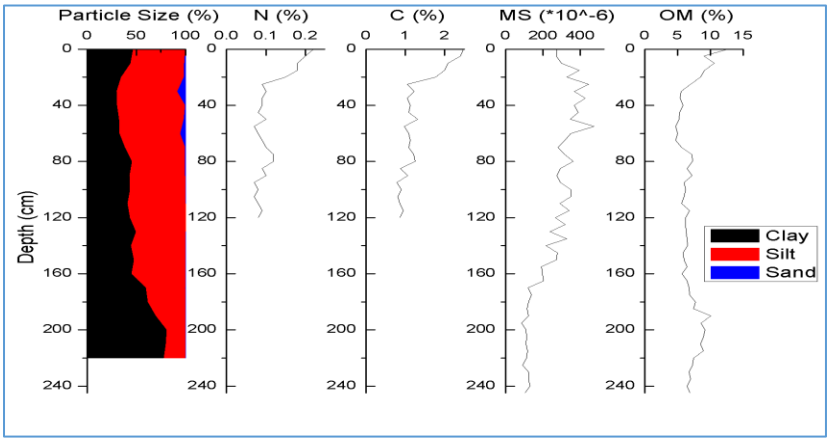

Figure 5.2 Particle size, N, C, MS, and OM results for sample site MS.SC02

5.3 MS.SC03

Figure 5.3 is a graphical depiction of results for the MS.SC03 sediment core, which was collected in a backswamp environment in St. Catherine Creek NWR, Mississippi. MS.SC03 mainly consists of equal amounts of clay and silt particles in the upper 80 cm, below which the clay fraction increases. The highest values for N (0.28%) and C (6.34%) occur at a depth of 115 cm. A marked decrease of N and C is observed between 0 and 20 cm, and N (0.1%) and C (1.08%) values generally remain constant between 20 and 75 cm depths. Both N (0.24%) and C (6.34%) values increase below 80 cm and reach their greatest values at 115 cm. MS values range from 81 * 10^{-6} to 382 * 10^{-6}. High MS values are observed between 75 and 90 cm region and recorded peak occurs at 85 cm below the surface. From 115 cm to 145 cm low values average 89 * 10^{-6}. OM percentage at the surface is 9.1% and averages 8.1% to a depth of 90 cm. A general increase of OM is observed between 95 and 145 cm. The greatest OM percentage of 20% occurs at a depth of 90 cm.

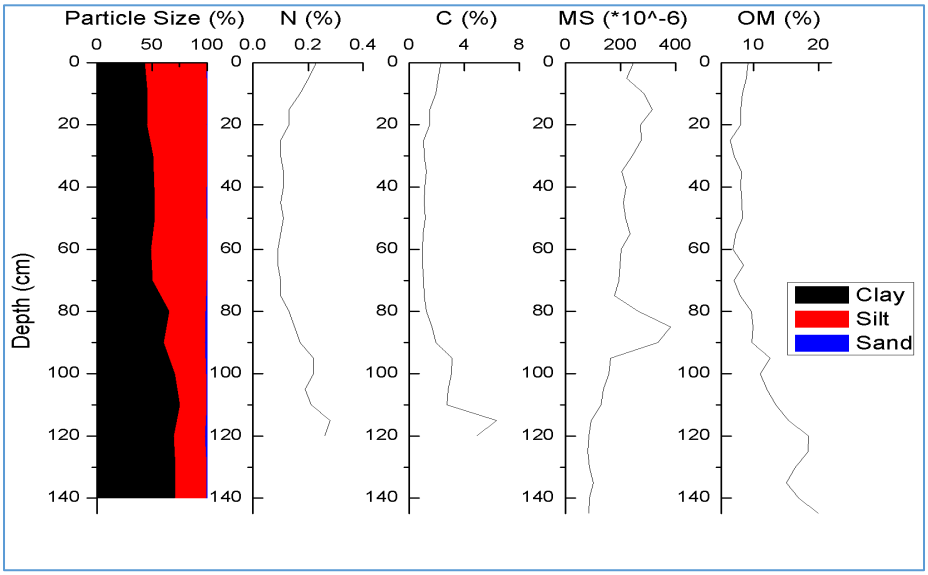

Figure 5.3 Particle size, N, C, MS, and OM results for sample site MS.SC03.

5.4 MS.SC04

Figure 5.4 is a graphical depiction of results for the MS.SC04 sediment core, which was collected in a backswamp environment in St. Catherine Creek NWR, Mississippi. The particle size distribution of MS.SC04 is dominated by clay and silt particles. A minor fraction of sand (12%) occurs at a depth of 10–40 cm. N and C concentrations follow a similar pattern and the greatest values of 0.18% and 2.07%, respectively, occur at a depth of 5 cm. After an initial decrease of N and C values from 0–20 cm, both N and C remain constant at average values of 0.08% and 1.0%, respectively. The greatest MS value of 460 * 10^{-6} occurs at a depth of 45 cm and the lowest value of 202 * 10^{-6} occurs at a depth of 85 cm. The average MS value was 357 * 10^{-6}. The greatest OM content of 7.9% occurs at a depth of 5 cm. From 5–25 cm a general decrease of OM from 7.9% to 3.5% is observed. From 25–150 cm OM values do not vary much around an average value of 4.4%.

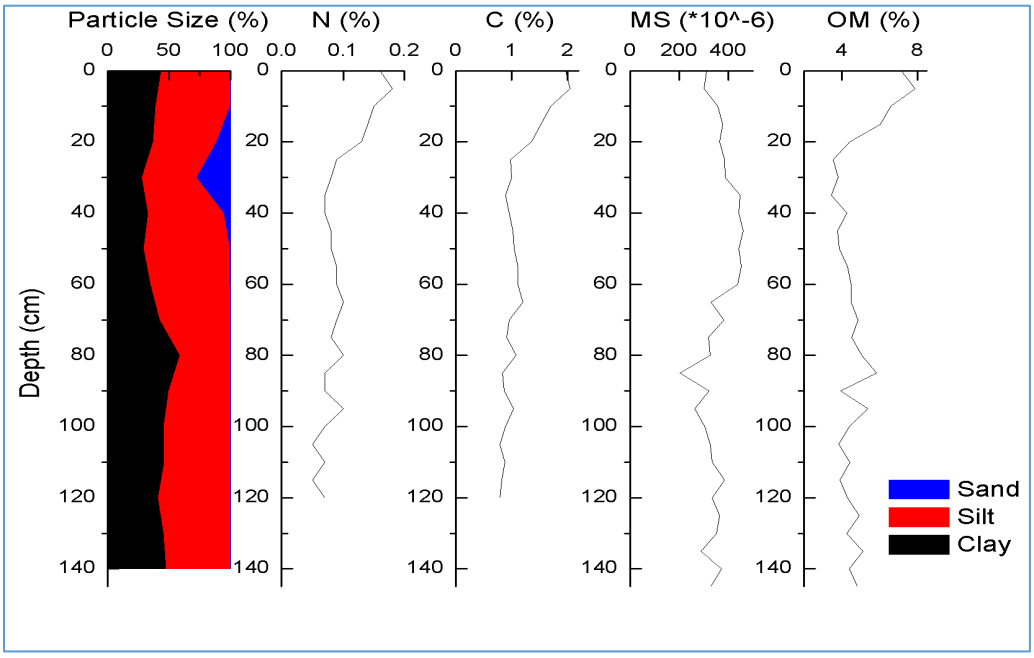

Figure 5.4 Particle size, N, C, MS, and OM results for sample site MS.SC04.

5.5 MS.CAT05

Figure 5.5 is a graphical depiction of results for the MS.CAT05 sediment core, which was collected in a backswamp environment in Cat Island NWR, Louisiana. Clay and silt particles dominate the particle size distribution and clays are the primary fraction between 60 and 145 cm depth below the surface. N and C have their greatest percentage values at the surface and decrease through the top 15 cm to relatively constant values. The greatest N concentration is 0.67% and decreases to 0.12% at 15 cm depth. The average N concentration between 15 and 125 cm is 0.09%. The greatest C concentration is 10.79% at the surface and remains relatively constant at 0.9% from 15–125 cm depth. The lowest MS value of 97 * 10^{-6} occurs at a depth of 75 cm and the highest value of 147 * 10^{-6} occurs at about 20 cm depth. The average MS value of the core is 126 * 10^{-6}. The greatest OM value of 16.4% occurs at the surface and it decreases to 6.5% at 10 cm. From 10–145 cm depth OM content remains relatively constant and averages 6.0%. The lowest value for OM (3.7%) occurs at a depth of 45 cm.

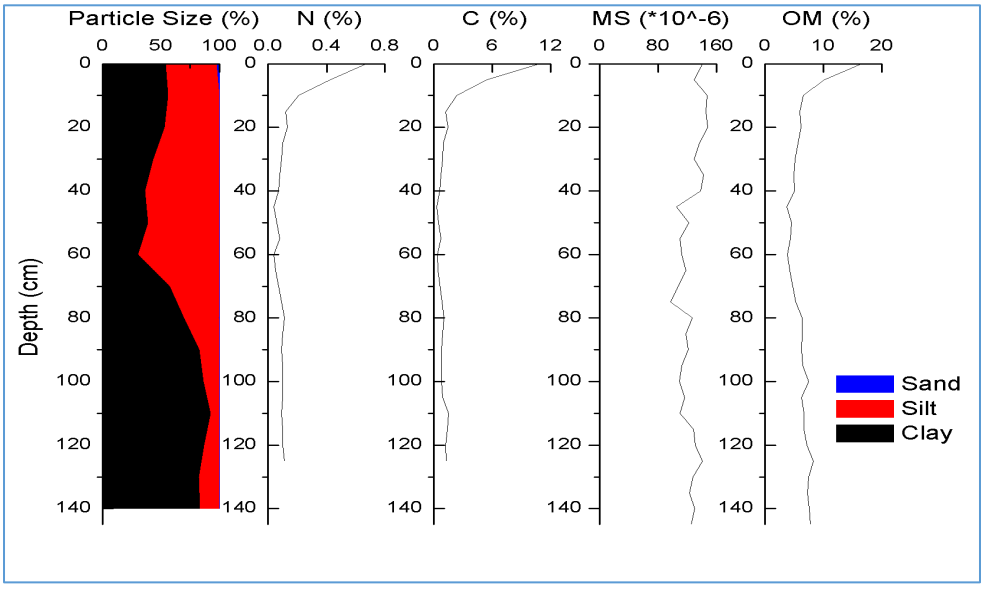

Figure 5.5 Particle size, N, C, MS, and OM results for sample site MS.CAT05.

5.6 MS.CAT06

Figure 5.6 is a graphical depiction of results for the MS.CAT06 sediment core, which was collected in a meander scroll (point-bar ridge and swale) environment in Cat Island NWR, Louisiana. The depth interval 0–120 cm mainly consists of equal fractions of clay and silt particles. However, the clay fraction increases from 120–145 cm. Both N and C have greatest values at the surface, 0.59% and 7.42%, respectively. N and C percentage values decrease to 0.14% and 1.38%, respectively, at a depth of 10 cm. Between 10 and 125 cm both N and C remain relatively constant with an average N value of 0.1% and average C value of 1.0%. The lowest MS value of 105 * 10^{-6} occurs at a depth of 140 * 10^{-6} cm and the greatest MS value of 304 * 10^{-6} occurs at a depth of 10 cm. The average MS value of the core is 195 * 10^{-6}. The OM graph follows a similar pattern to N and C. The greatest OM value is 12.5% at the surface. OM values decrease to 6.1% at 10 cm and maintain a relatively constant value averaging 5.6% between 10 and 145 cm.

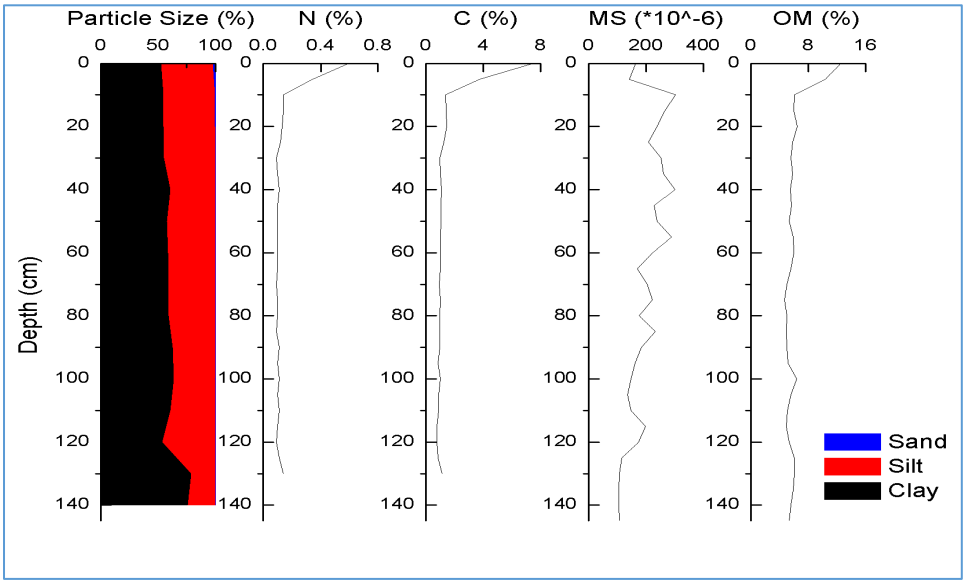

Figure 5.6 Particle size, N, C, MS, and OM results for sample site MS.CAT06.

5.7 MS.CAT07

Figure 5.7 is a graphical depiction of results for the MS.CAT07 sediment core, which was collected along a natural levee backslope on private property along Cat Island Road, Louisiana. The particle size distribution of the sediment core is dominated by silt and sand particles. The clay fraction remains constant at about 25% for the entire core. The average sand fraction is 30% and the greatest sand fraction of 47.5% occurs at 30 cm. The greatest concentrations of N and C, 0.18% and 2.27%, respectively, occur at the surface. Following an initial drop of N and C values to 0.04% and 0.52% at a depth of 25 cm, N and C values remain constant between 25 and 120 cm. From 25–120 cm N averages 0.03% and C averages 0.6%. The lowest N value of 0.02% occurs between 65 and 80 cm whereas the lowest value for C (0.41%) occurs at a depth of 65 cm. The greatest MS value of 756 * 10^{-6} occurs at 125 cm depth and the lowest MS value of 305 * 10^{-6} occurs at 145 cm. The average MS value for the MS.CAT07 sediment core is 440*10^{-6}. The OM graph follows a relatively similar pattern to the N and C graphs, but below the 125 cm depth OM values increase to 145 cm. The highest OM value of 6.6% occurs at the surface and decreases to 2.7% at 20 cm depth. From 20–125 cm depth OM values average 2.6%. Between 125 and 145 cm OM values increase from 2.2% to 4.5%.

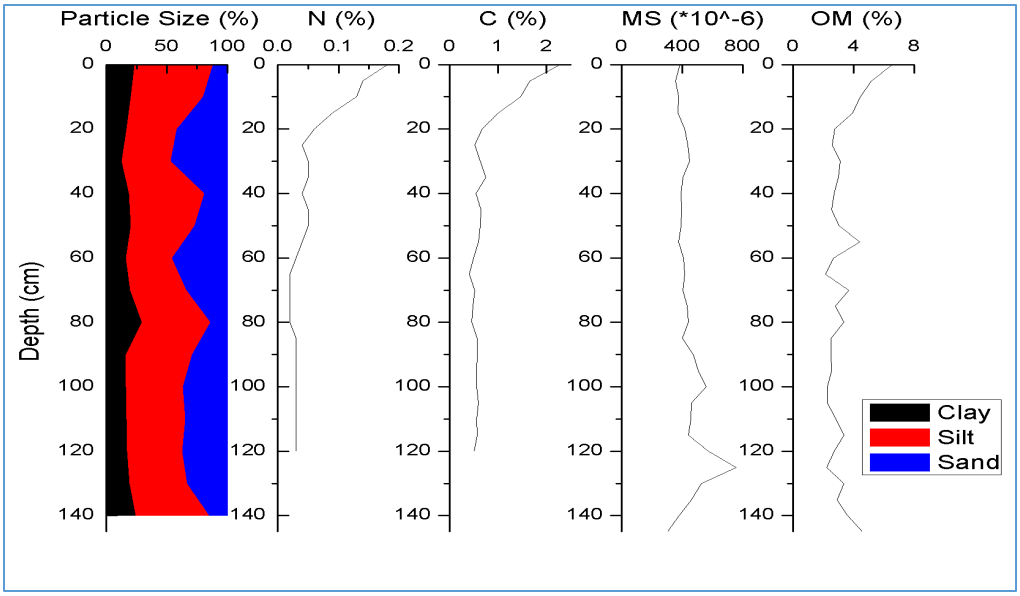

Figure 5.7 Particle size, N, C, MS, and OM results for sample site MS.CAT07.

5.8 MS.SC08

Figure 5.8 is a graphical depiction of results for the MS.SC08 sediment core, which was collected in a swale of a meander scroll (point-bar ridge and swale) environment in St. Catherine Creek NWR, Mississippi. The sediment core mainly consists of clay and silt particles. Between 40 and 140 cm the clay fraction is greater relative to the silt fraction. The greatest N (0.44%) and C (4.09%) concentrations occur at the surface. N and P concentrations decrease to 0.14% and 1.33% at 10 cm depth, respectively, and remain relatively constant between 10 and 55 cm. From 60–95 cm depth both N and C percentages have a secondary peak and remain constant at low values between 100 and 140 cm depth. The greatest MS value of 240 * 10^{-6} occurs at a depth of 20 cm, and the lowest MS value of 81 * 10^{-6} occurs at 65 cm depth. The average MS value for the MS.SC08 sediment core is 122 * 10^{-6}. From 0–50 cm OM values are relatively constant and average 6.5%. High OM values occur between 55 and 100 cm and

the highest value of 9.9% occurs at 80 cm depth. From 105–145 cm OM values again decrease to an average of 6.2% and remain relatively constant.

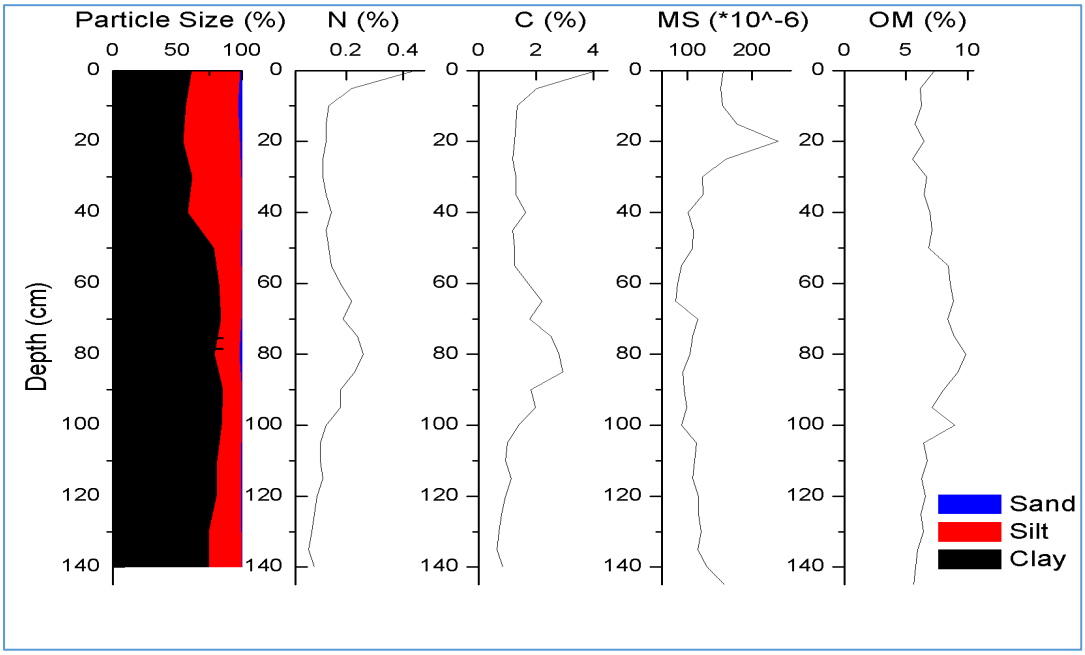

Figure 5.8 Particle size, N, C, MS, and OM results for sample site MS.SC08.

5.9 Phosphorus Results

Phosphorus (P) was analyzed for five of the eight available cores (Figure 5.9). MS.SC01 has relatively constant P levels; the highest value of 0.08% occurs at the surface and averages 0.05% from 10–90 cm. MS.SC03 has relatively constant P levels averaging 0.07% from 0–75 cm and increases to an average of 0.13% between 75 and 95 cm. From 100–120 cm P decreases to relatively low constant values averaging 0.06%. P concentrations for MS.SC04 range between 0.04% to 0.08%. The greatest value occurs at a depth of 5 cm and the lowest P level occurs at 40 cm. The average P value for the MS.SC04 sediment core was 0.06%. MS.CAT07 has relatively low constant P concentrations averaging 0.05%. The highest P concentrations occur in sediment core

MS.SC08 with a maximum of 0.20% at the surface. The P concentration decreases from the surface to 0.04% at 40 cm depth. A general increase in P values occurs between 45 and 80 cm before declining again to relatively low values between85 and 100 cm. Finally, P concentrations again increase from 0.07%to 1.1% from 100–145 cm, respectively.

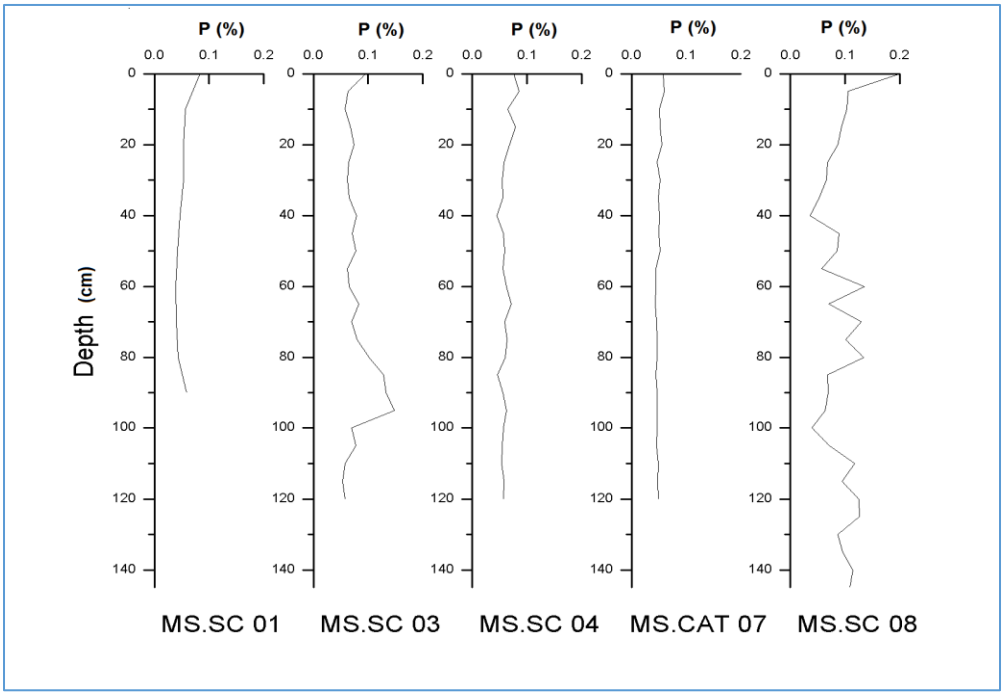

Figure 5.9 Phosphorus results for sample sites MS.SC01, MS.SC03, MS.SC04, MS.CAT07, and MS.SC08.

CHAPTER VI – DISCUSSION

6.1 MAGNETIC SUSCEPTIBILITY (MS)

Magnetic susceptibility (MS) is used in this study as a qualitative indicator of sediment composition in the study areas. *Sensu stricto*, MS quantifies the ease by which bulk sediments can be magnetized. *Sensu lato*, MS is an indicator for the quantity of certain detrital constituents (i.e., mineralogy) deposited in the floodplain environment. In general, MS values for sediment are considered high if values exceed $3 * 10^{-7}$ (e.g., Ellwood et al., 2006). MS values vary with depth for all sediment cores (Figure 6.1) and all have high MS values. A summary of MS values is available in Table 6.1. The lowest MS values among all the sediment cores occur at MS.CAT05 and MS.SC08, and MS values at both of these locations do not vary with depth as compared to other cores. The greatest average MS values and greatest range of MS values within the core occurs at the MS.CAT07 levee backslope deposit. The range of MS values for all backswamps except for MS.CAT 05 have high values whereas both point-bar deposits have minor variation with depth.

Table 6.1

Summary of MS values of the sediment cores

	MS.SC 01	**MS.SC 02**	**MS.SC 03**	**MS.SC 04**	**MS.CAT 05**	**MS.CAT 06**	**MS.CAT 07**	**MS.SC 08**
Maximum	590	472	382	461	148	304	757	240
Minimum	242	84	81	202	97	105	305	81
Range	348	388	301	259	51	198	452	159
Average	348	251	197	357	126	194	440	122

(MS values should be multiplied by $(10)^{-6}$)

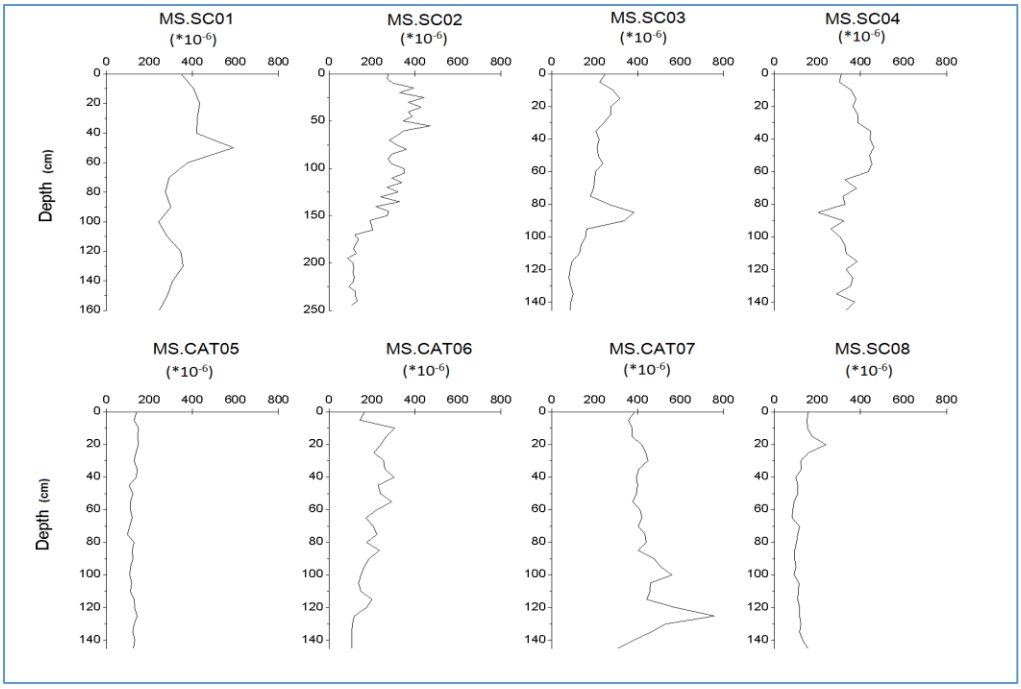

Figure 6.1 MS values with depth for all sample sites.

Backswamp deposits – MS.SC01, MS.SC02, MS.SC03, MS.SC04 and MS.CAT05; Point-bar deposits–MS.CAT06 and MS.CAT08; Levee backslope deposit.

Figure 6.2 graphically displays MS variability with the clay percentage for depth increment samples in all sediment cores. There is a strong negative linear correlation between MS and clay percentage; the Pearson correlation value is -0.778 ($P<0.01$, $N=111$). Composition of the clay plays a major role in determining MS values. Most of the clay in the study area can be rich in kaolinite which has low MS values. Another possibility to explain this negative correlation is the iron reduction. Most of the sediment cores have greater clay content at deeper levels below about depth of 100 cm, which is frequently below the water table. Iron reduction under such anaerobic conditions might have an effect on lowering the MS values associated with higher clay content

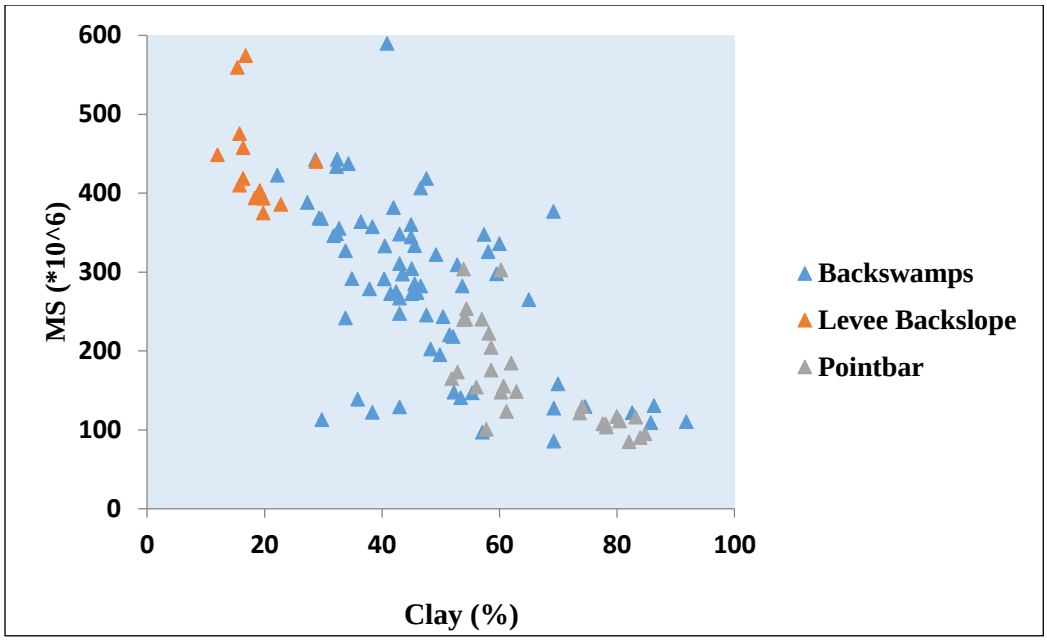

Figure 6.2 MS values and clay percentage values for all sediment cores

(Number of data points = 111)

6.2 ORGANIC MATTER (OM)

Figure 6.3 summarizes variability of organic matter (OM) as a function of depth for all sediment cores. OM in the upper 10 cm of all locations ranges from 6.6% to 16.4%. For the upper 10 cm, all sediment cores from St. Catherine Creek NWR have close to 10% or less OM whereas the same interval in MS.CAT05 and MS.CAT06 from Cat Island NWR has relatively high OM percentages. The lowest value for the upper 10 cm occurs at MS.CAT07.

St. Catherine Creek sample sites were located at approximately the same elevation and have similar surface vegetation except for MS.SC03. All the St Catherine Creek sediment samples have relatively similar OM concentration at the topsoil. Therefore, surface vegetation can be a factor in determining the OM concentration in the topsoil as ground cover vegetation best preserves OM in the upper 10 cm. In the Cat Island NWR

study area, MS.CAT05 and MS.CAT06 were located at similar elevations but MS.CAT07 occurs at a relatively high elevation along the levee backslope. The highest observed seed line that represents the water surface during the Summer 2015 flood was 3.2 m above the surface in the vicinity of MS.CAT05, where as it was 35 cm above the ground surface at MS.CAT07. Therefore elevation of the sample site plays an important role determining the OM concentration because low elevations tend to be more saturated and less oxidized, and thus, OM preservation potential is greater.

Most of the sediment cores do not have much variation of OM with depth except for MS.SC03 and MS.SC08. Comparatively high OM content occurs at MS.SC03 below 100 cm depth. During the field data collection trip, 100 cm was the water-table depth at this location and fibrous woody tissues were recovered at a depth of 115 cm. Microbial decomposition, which is the primary process for breakdown of OM, is hindered by lack of oxygen in the strongly anaerobic conditions. Thus, high OM values at deeper levels in MS.SC 03 are associated with anaerobic conditions that retard OM decomposition. MS.SC 08 is from a point-bar swale deposit and relatively high OM concentrations occur at between 50 and 100 cm. According to Brady and Weil (2008), fine-textured soils have high OM content because more of the organic material is protected from decomposition by being bound in clay-humus complexes. Particle size analysis results indicate that the marked increase in clay corresponds with the depth region of MS.SC 08 with a high OM content.

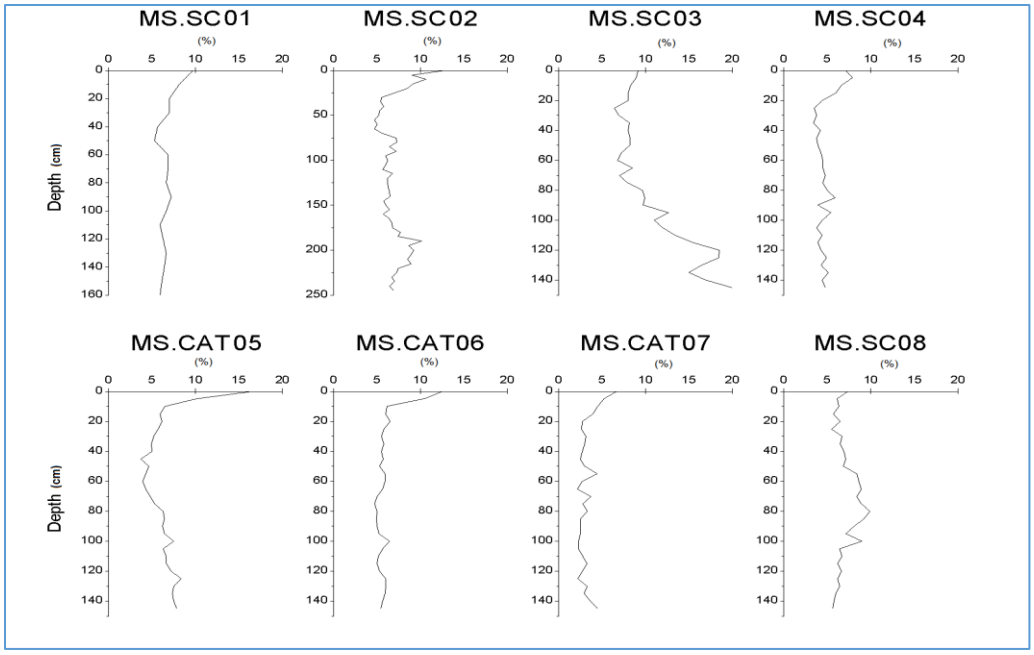

Figure 6.3 OM values with depth for all sample sites.

Backswamp deposits – MS.SC01, MS.SC02, MS.SC03, MS.SC04 and MS.CAT05; Point-bar deposits–MS.CAT06 and MS.CAT08; Levee backslope deposit – MS.CAT07.

Table 6.2 summarizes OM values in the study area. The highest average OM value occurs at the MS.SC03 backswamp deposit. The lowest average values and the least variation among the values occur at the MS.SC07 levee backswamp deposit, which consists mainly of silt and sand particles. High ranges of values are observed in both MS.SC03 and MS.CAT05.

Table 6.2

Summary of OM values in the study area.

	MS.SC 01	MS.SC 02	MS.SC 03	MS.SC 04	MS.CAT 05	MS.CAT 06	MS.CAT 07	MS.SC 08
Maximum	9.7%	12.6%	20.0%	7.9%	16.4%	12.5%	6.6%	9.9%
Minimum	5.3%	4.7%	6.4%	3.4%	3.7%	4.7%	2.1%	5.5%
Range	4.4%	7.9%	13.6%	4.5%	12.7%	7.8%	4.5%	4.4%
Average	6.7%	7.0%	10.8%	4.7%	6.5%	6.0%	3.2%	7.1%

Figure 6.4 and figure 6.5 graphically display the variance of OM values with clay percentage and MS values. A moderate positive linear correlation with a 0.490 ($P<0.01$, $N=111$) Pearson correlation value is observed between OM and clay percentage. Within a local landscape soil texture is an important factor often responsible for marked differences in OM along with other factors such as temperature, moisture, vegetation, drainage effects, and land use patterns (Brady and Weil, 2008). OM and MS have a moderate negative linear relationship with a Pearson correlation value of -0.472 ($P<0.01$, $N=199$). This is due to the fact that OM belongs to the diamagnetic materials which have a weak negative susceptibility (Dearing, 1994). High OM content tends to reduce the overall positive magnetic response in the presence of a magnetic field.

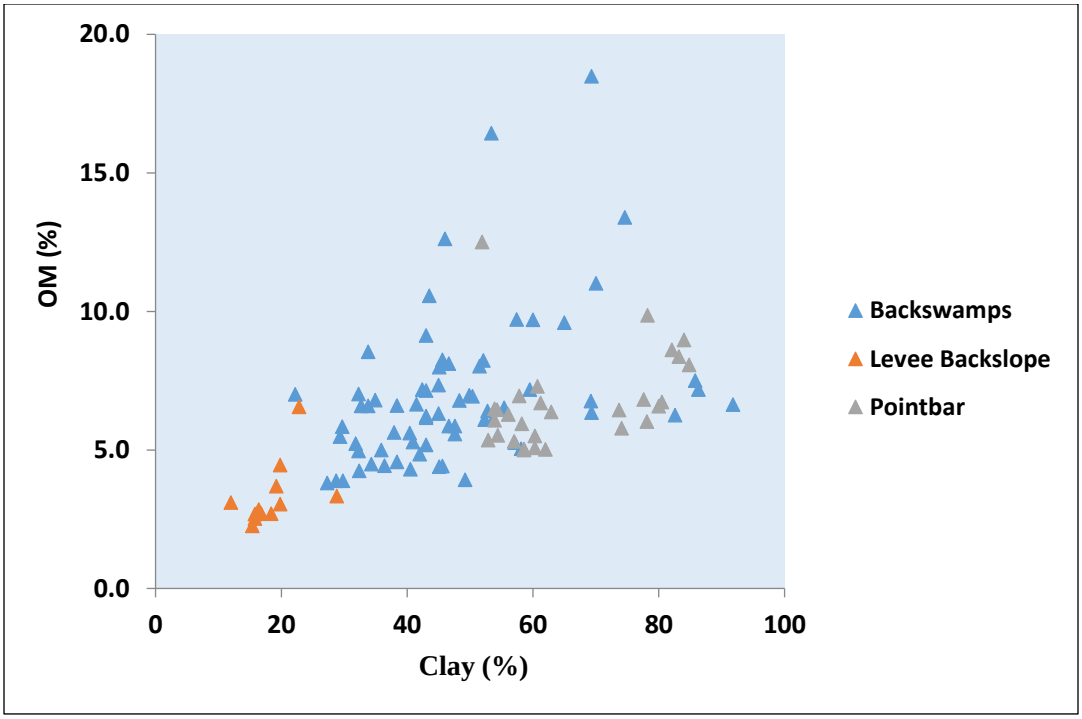

Figure 6.4 OM values and clay percentage values of all sediment cores

(N=111)

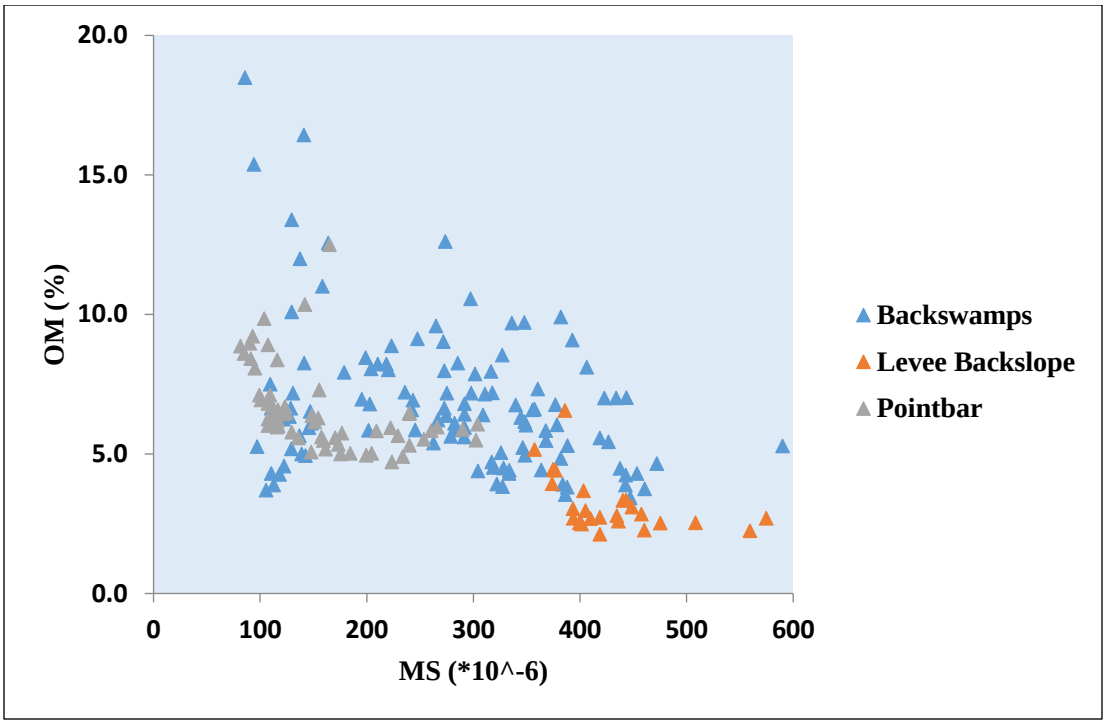

Figure 6.5 OM values and MS values of all sediment cores.

(N=199)

6.3 SEDIMENT PARTICLE SIZE

Figure 6.6 summarizes variability of clay, silt and sand particles with depth for each sediment core. All cores have more combined clay and silt than sand. The MS.CAT07 core from a levee backslope deposit, which is the closest sample location to the main river channel, has a high sand fraction relative to other sediment cores. Similarly, MS.SC05 and MS.SC08, which have the greatest distance between the sample site and the main river channel, have high clay fraction relative to other sediment cores. Size of the deposited sediment is greatly depends on the energy of the water. Sample sites closer to the river received high velocity overbank floods in comparison to the sites have a greater distance from the main channel.

The MS.SC01 backswamp deposit has alternative layers of high clay and high silt fractions. All other backswamp deposits have a gradually increasing clay percentage with depth except for MS.CAT05, which has a minimum clay content at about 60 cm and then abruptly increases below 60 cm. The MS.CAT06 point-bar deposit has relatively constant clay and silt fractions throughout the core until the clay fraction increases below 120 cm.

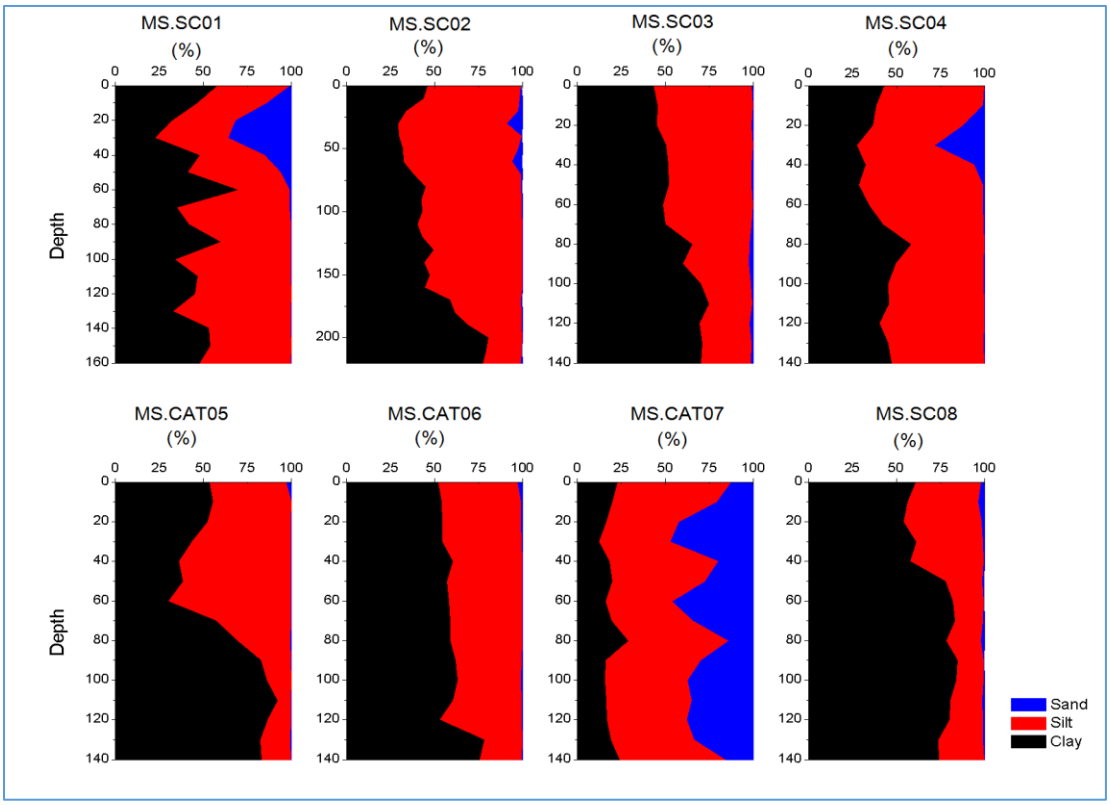

Figure 6.6 Particle size fractions of all the sediment core samples.

6.4 CARBON (C)

Figure 6.7 graphically displays C variance with depth, and all sediment cores have relatively high C values near the ground surface that taper off to low constant values at a depth of no more than 25 cm below ground. All sediment cores from St. Catherine Creek NWR have relatively similar C concentrations in the upper 25 cm. MS.CAT 05 and MS.CAT 06 from Cat Island NWR show relatively high C concentrations in the upper 25

cm whereas MS.CAT 07 has the lowest C concentration values in the upper 25 cm. These trends are similar to the previously discussed OM concentration variations. Only the MS.SC 03 backswamp deposit and the MS.SC 08 point-bar deposit exhibit considerable variation with depth. Changes in C concentrations in both MS.SC 03 and MS.SC 08 correspond with variations in OM concentration.

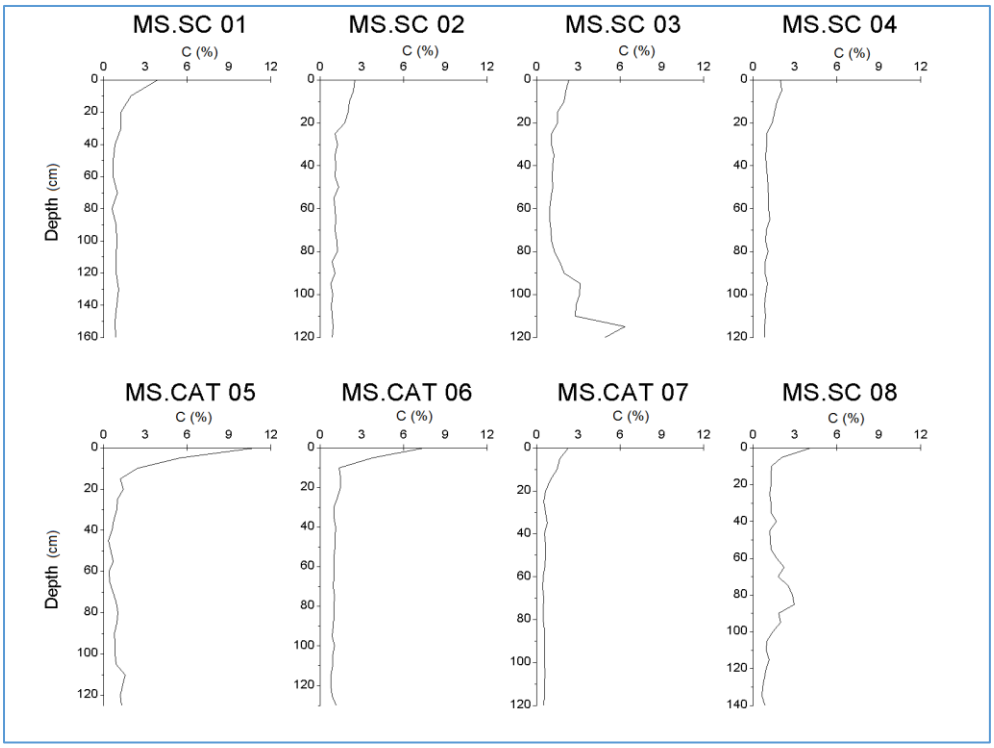

Figure 6.7 Carbon (C) concentrations with depth for all sediment core samples.

Table 6.3 summarizes C concentration values and the approximate depths at which C is sequestered in the upper sediment column before it is degraded into various end products. The greatest range of values occurs at MS.CAT 05 and lowest value range occurs at MS.CAT 07.

Table 6.3

Summary of C concentrations in the study area.

	MS.SC 01	MS.SC 02	MS.SC 03	M.SC 04	MS.CAT 05	MS.CAT 06	MS.CAT 07	MS.SC 08
Maximum	3.84%	2.47%	6.34%	2.04%	10.79%	7.42%	2.27%	4.09%
Minimum	0.60%	0.79%	0.95%	0.79%	0.33%	0.46%	0.50%	0.63%
Range	3.24%	1.68%	5.39%	1.25%	10.46%	6.96%	1.77%	3.46%
Average	1.14%	1.26%	2.00%	1.11%	1.53%	1.37%	0.70%	1.56%
Sequestered depth	20 cm	25 cm	15 cm	25 cm	15 cm	10 cm	25 cm	10 cm

Figure 6.8A graphically displays the relationships between C concentrations and OM. Figure 6.8 B, C, and D graphically display the same relationship for the subset of sediment samples from different sub-environments within the study area. There is a strong positive relationship between C concentrations and OM content for all the measured sediments in the study area and the same relationship is observed for the sediment samples from different sub-environments. Pearson correlation values for all aforementioned relationships are provided in Table 6.4. A strong correlation between OM and C indicates that OM is the primary source for C in the study area. Therefore it is safe to assume that variations of C in the MS.SC03 and MS.SC08 sediment cores are mainly because of OM variations.

Table 6.4

Correlation coefficient values for relationships between carbon and organic matter.

	All samples (N=198)	Backswamp (N=117)	Point-bar (N=56)	Levee backslope (N=25)
Pearson correlation coefficient	0.763	0.776	0.801	0.888

graphically displayed in Figure 6A–D.

($P<0.01$) for all the values.

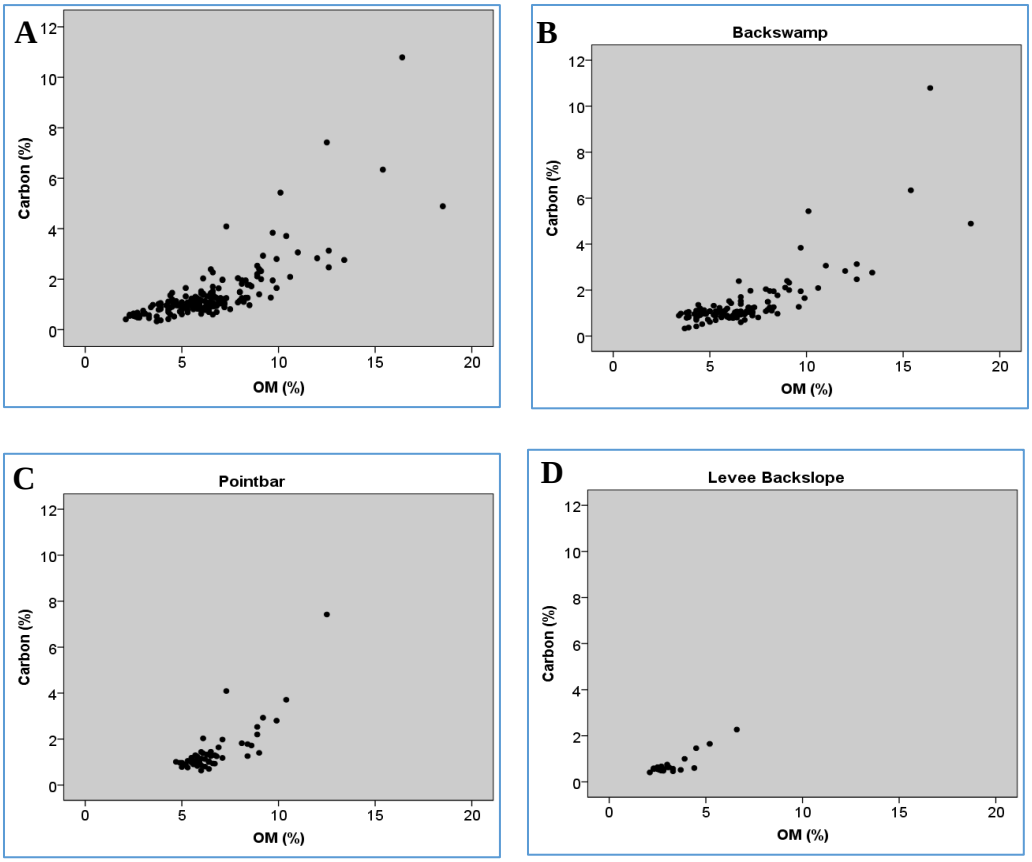

Figure 6.8 Relationship between C and OM for sediment samples.

(A) Relationship between C and OM for all sediment samples (N=198). (B) Relationship between C and OM for sediment samples from backswamp deposits (N=117). (C) Relationship between C and OM for sediment samples from point-bar deposits (N=56). (D) Relationship between C and OM for sediment samples from levee backslope deposits (N=25).

Figure 6.9 graphically displays the relationships between C concentrations and clay percentage. There is not an apparent correlation between C and clay content with the correlation coefficient for all sediment samples only being 0.198. The highest correlation coefficient within the sub-environments was for the levee backslope samples, which was 0.300. Sediment samples from point-bar deposits have a low negative correlation of -0.132. The correlation coefficient for the backswamp deposit sediments is 0.187. Table 6.5 provides Pearson correlation values including transformed clay percentage values. All values have low correlation with C content.

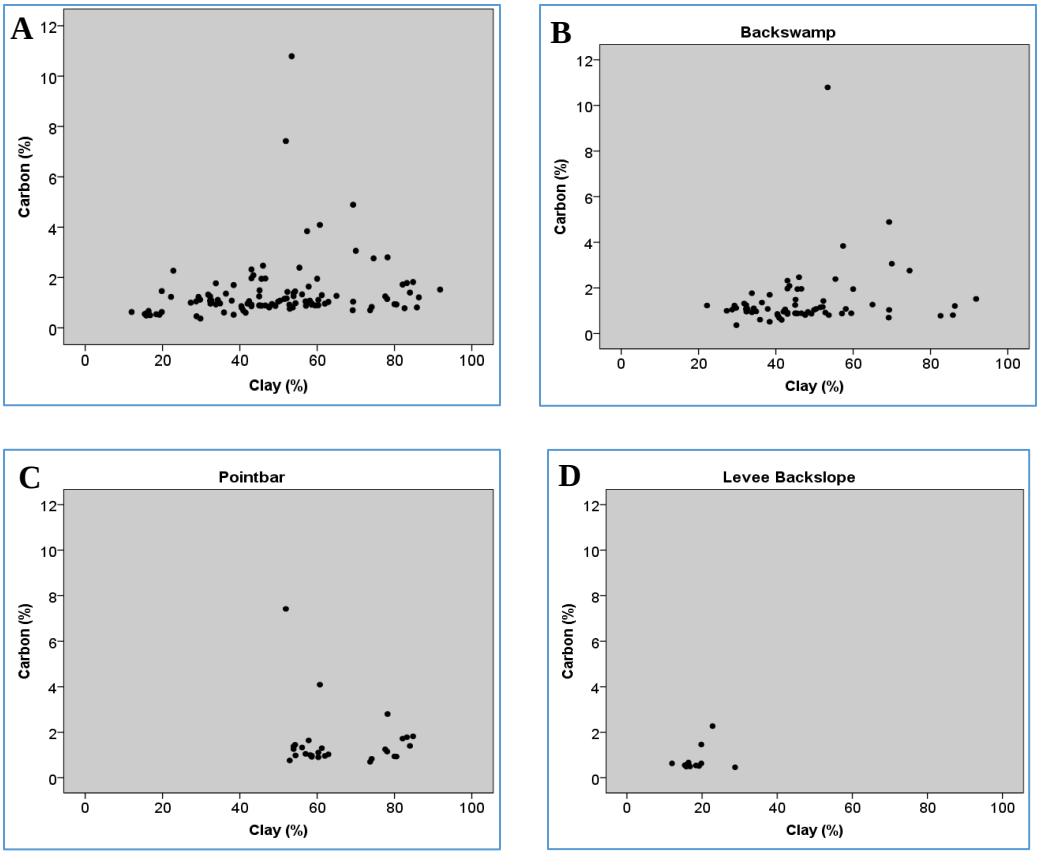

Figure 6.9 Relationship between C and clay percentage for sediment samples.

(A) Relationship between C and clay percentage for all sediment samples. (B) Relationship between C and lay percentage for sediment samples from backswamp deposits. (C) Relationship between C and clay percentage for sediment samples from point-bar deposits. (D) Relationship between C and clay percentage for sediment samples from levee backslope deposits.

Table 6.5

Pearson correlation values for relationships between carbon (C) and transformed values of clay content.

	$(clay)^2$	**$exp^{(clay)}$**	**1/(clay)**	**ln (clay)**
C for all sediments (N=111)	0.158	0.01	-0.229*	0.226*
C in backswamp sediments (N=69)	0.156	0.007	-0.209	0.207
C in point-bar sediments (N=29)	-0.116	0.034	0.168	-0.149
C in levee backslope sediments (N=13)	0.253	-0.169	-0.338	0.331

* - ($P < 0.05$) all the other values have ($P > 0.05$)

Figure 6.9 graphically displays the relationships between C concentrations and MS values. There is a low negative correlation between C and MS. Generally, high MS values are associated with constant low C values. The correlation coefficient for all sediment samples is -0.273 (P<0.01, N=198). The highest correlation coefficient value of –0.436 (P<0.05, N=25) is associated with the levee backslope deposits. Backswamps and point-bar deposits have a correlation coefficient of -0.224 (P<0.05, N= 117) and -0.160 (P>0.05, N=56), respectively. Pearson correlation values of C with the transformed MS values provided in Table 6.6 indicate low correlation between C and MS.

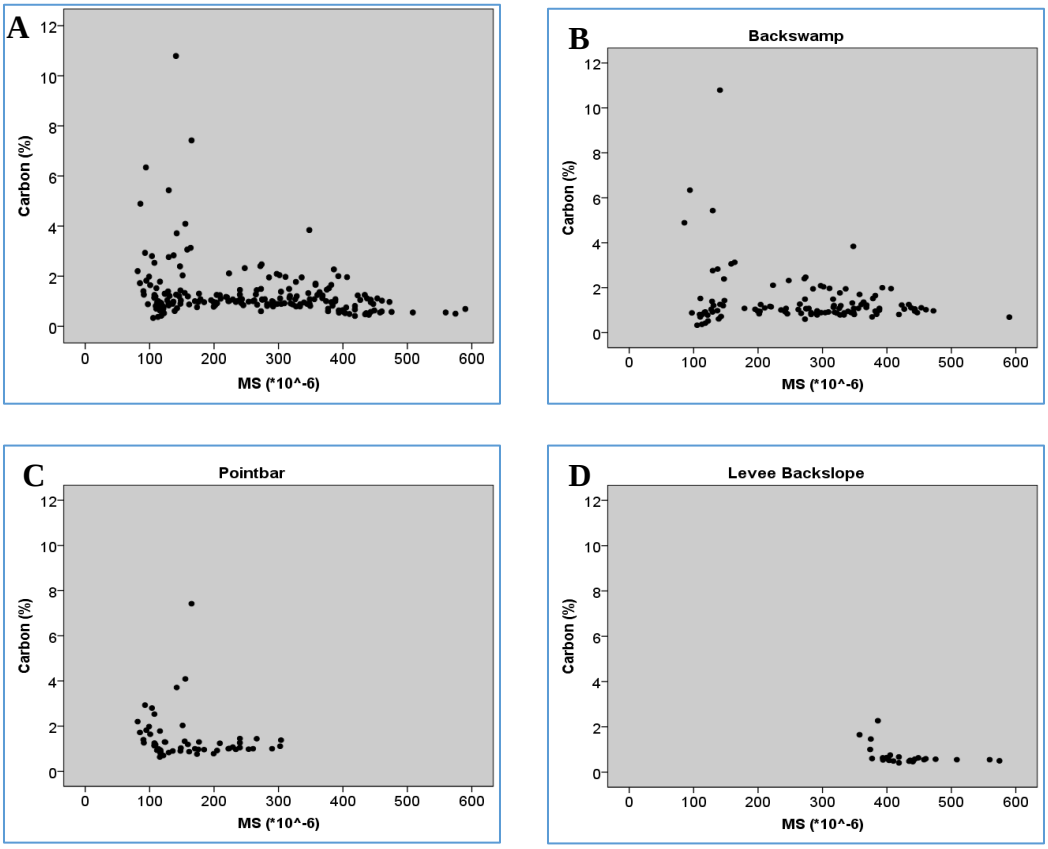

Figure 6.10 Relationship between C and MS for all sediment samples.

(A) Relationship between C and MS for all sediment samples. (B) Relationship between C and MS for sediment samples from backswamp deposits. (C) Relationship between C and MS for sediment samples from point-bar deposits. (D) Relationship between C and MS for sediment samples from levee backslope deposits.

Table 6.6

Pearson correlation values for relationships between carbon (C) and transformed values of magnetic susceptibility (MS).

	$(MS)^2$	$exp^{(MS)}$	1/(MS)	ln (MS)
C for all sediments (N=198)	-0.265**	.000	.262**	-0.271**
C in backswamp sediments (N=117)	-0.204*	.000	.250**	-0.240**
C in point-bar sediments (N=56)	-0.161	-.022	0.149	-0.155
C in levee backslope sediments (N=25)	-0.403*	.000	0.499*	-0.468*

*- (P<0.01), **- (P<0.05), all the other values have P>0.05

6.5 NITROGEN (N)

Figure 6.11 graphically displays a strong statistical relationship between C and N with a Pearson correlation coefficient of 0.945 (P<0.01, N=198). Therefore, all the N variations with different parameters such as depth, OM, MS, and clay percentage are very similar to that of C. Figure 6.10 indicates that high percentages of both C and N are from a similar source that is most likely to be from OM.

Figure 6.12 graphically displays N variability with depth at each location. Similar to C, high N concentrations are sequestered near the ground surface. Compared to C concentrations, N concentrations are an order of magnitude lower. MS.CAT05 and MS.CAT06 from Cat Island NWR have comparatively high N concentrations in the upper 15 cm. The MS.SC03 backswamp deposit from St. Catherine Creek NWR has increasing N concentrations below 80 cm, which is similar to C and is associated with high OM content at that depth. Similarly, the MS.SC08 point-bar deposit has relatively high N concentrations between 60 and 100 cm that correspond with high OM content.

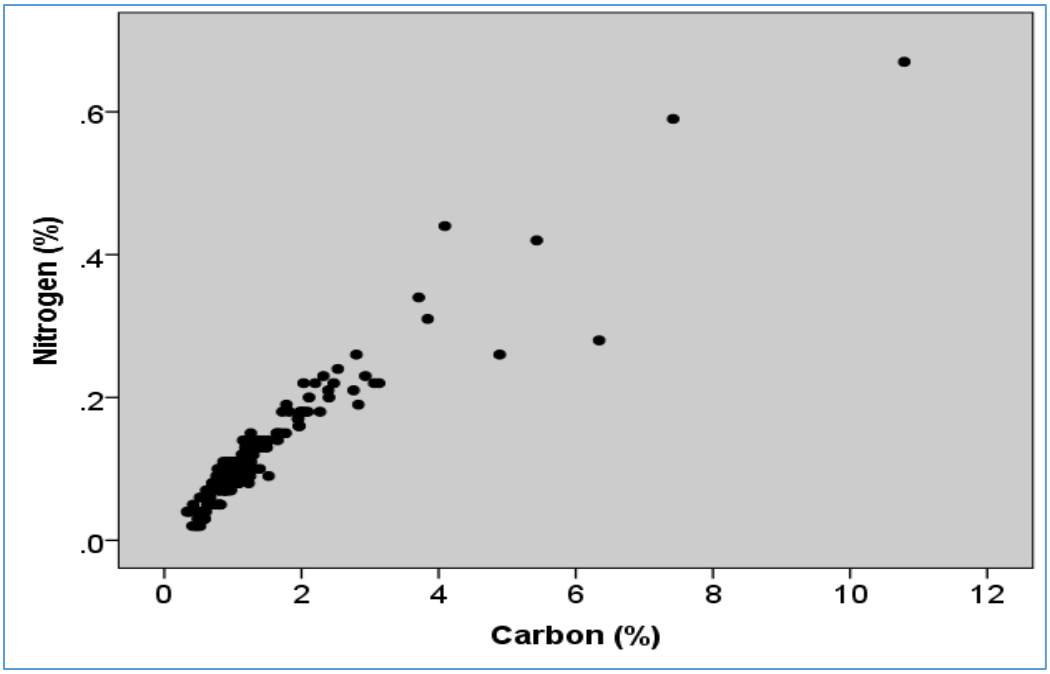

Figure 6.11 C concentration and N concentration values for all sediment cores.

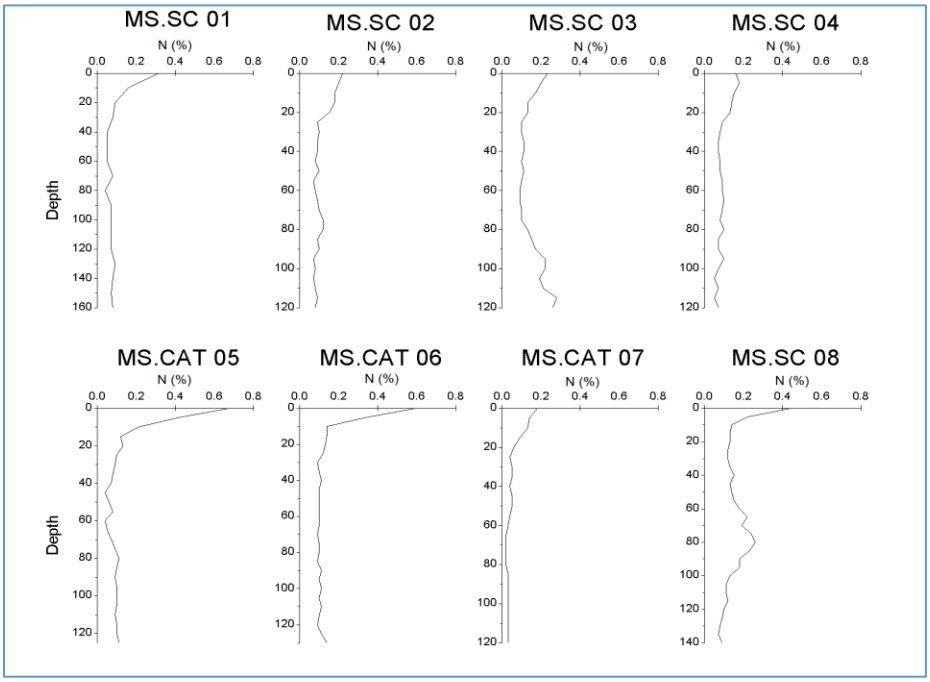

Figure 6.12 Nitrogen (N) concentrations with depth for all sediment-core samples.

Table 6.7 summarizes N concentration values and the approximate depths at which N is sequestered in the upper sediment column before it is degraded into various end products.

Table 6.7

Summary of N concentrations in the study area.

	MS.SC 01	MS.SC 02	MS.SC 03	MS.SC 04	MS.CAT 05	MS.CAT 06	MS.CAT 07	MS.SC 08
Maximum	0.31%	0.22%	0.28%	0.18%	0.67%	0.59%	0.18%	0.44%
Minimum	0.05%	0.07%	0.09%	0.05%	0.04%	0.09%	0.02%	0.07%
Range	0.26%	0.15%	0.19%	0.13%	0.63%	0.50%	0.16%	0.37%
Average	0.09%	0.11%	0.15%	0.09%	0.13%	0.13%	0.05%	0.16%
Sequestered depth	20 cm	25 cm	15 cm	25 cm	15 cm	10 cm	25 cm	10 cm

Figure 6.13 graphically displays the relationships between N concentrations and OM content. Similar to C, N and OM have a strong correlation and the same relationship is observed for the different sub-environments. Correlation coefficients are provided in Table 6.8. The highest correlation between N and OM is associated with sediment samples from levee backslope deposits along Cat Island road. Backswamp and point-bar deposits have relatively similar correlations for N and OM.

Table 6.8

Correlation coefficient values for relationships between nitrogen and organic matter

	All sediment samples (N=198)	Backswamp sediments (N=117)	Point-bar sediments (N=56)	Levee backslope sediments (N=25)
Pearson correlation coefficient	0.750*	0.759*	0.785*	0.856*

graphically displayed in Figure 11A–D

*($P<0.01$)

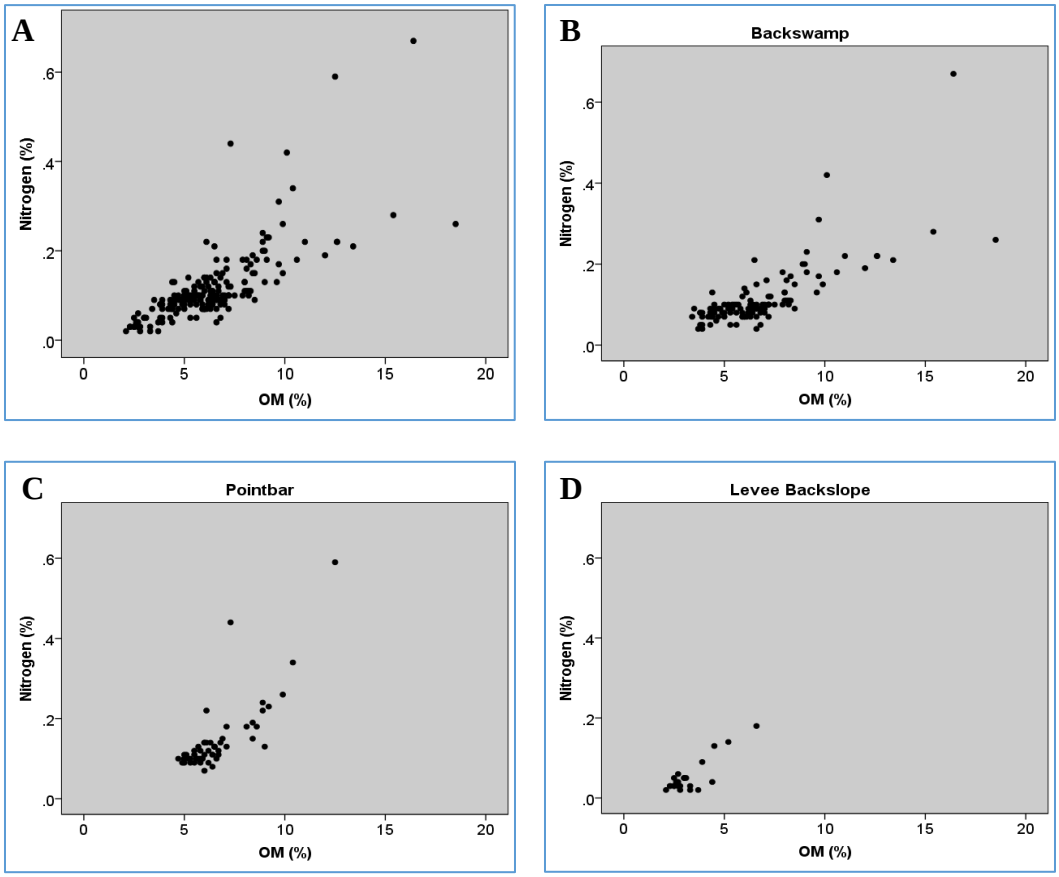

Figure 6.13 Relationship between nitrogen (N) and organic matter (OM) for sediment samples

(A) Relationship between nitrogen (N) and organic matter (OM) for all sediment samples. (B) Relationship between N and OM for sediment samples from backswamp deposits. (C) Relationship between N and OM for sediment samples from point-bar deposits. (D) Relationship between N and OM for sediment samples from levee backslope deposits.

N does not have a strong statistical relationship with clay percentage or with MS. Similar to C, N has a low positive correlation with clay percentage and low negative correlation with MS. Point-bar sediments do not have any relationship between N and clay percentage. Sediments from levee backslope deposits have the highest correlation between N and MS. Pearson correlation values for N with clay percentage and MS are

provided in Table 6.9. Additionally, correlation coefficient values of N and transformed clay and MS values are provided in Table 6.9.

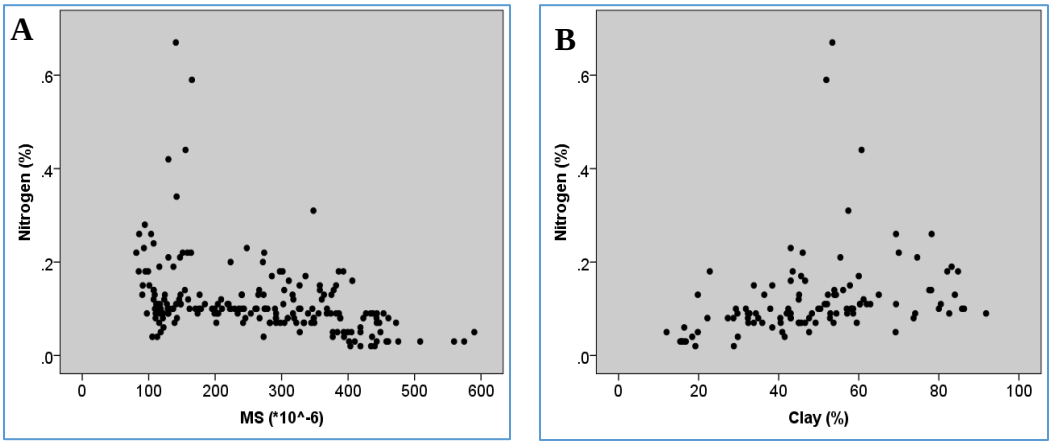

Figure 6.14 Nitrogen variations with clay and magnetic susceptibility.

(A) Relationship between nitrogen (N) and clay percentage for all sediment samples. (B) Relationship between N and magnetic susceptibility (MS) for all sediment samples.

Table 6.9

Pearson correlation values for nitrogen (N), clay percentage, and magnetic susceptibility (MS).

	All soil samples	**Backswamp soils**	**Pointbar soils**	**Levee backslope soil**
N and Clay	0.301**	0.205	-0.081	0.242
N and $(Clay)^2$	0.251**	0.163	-0.068	0.194
N and $exp^{(Clay)}$	- 0.030	-0.039	0.039	-0.212
N and 1/Clay	-0.331**	-0.249*	0.112	-0.282
N and ln(Clay)	0.334**	0.236	-0.096	0.273
N and MS	-0.388**	-0.246**	-0.205	-0.483*
N and MS^2	-0.387**	-0.242**	-0.206	-0.448*
N and exp^{MS}	0.000	0.000	-0.023	0.000
N and 1/MS	0.343**	0.223*	0.187	0.551
N and ln (MS)	0.372**	-0.238**	-0.198	-0.518**

*- (P<0.01), **-(P<0.05) all the other correlation values are not significant.

6.6 PHOSPHORUS (P)

Phosphorus was analyzed for only five of the eight available sediment cores. In contrast to C and N, P has little variation with depth at each location. Levee backslope deposits of MS.CAT07 and backswamp deposits of MS.SC 1 and MS.SC03 have relatively constant P concentrations throughout the measured depths. Reduced solubility of P in comparison to C and N might be the reason for little variation with depth (Schonbrunner et al., 2012; Brady and Weil, 2008). Therefore, leaching losses of P is generally low. Some variability with depth is observed for N concentrations in the MS.SC03 backswamp and MS.SC08 point-bar sediment samples. High OM and clay percentage values correspond with the high P concentrations.

Figure 6.15 and figure 6.16 graphically display the relationships between P concentrations and OM content. P concentrations exhibit less correlation with OM in comparison to C and N whose concentrations are more dependent on OM content. Unlike C and N, organic P is not the predominant source for available P in the study areas. Point-bar sediments do not have any correlation between P and OM. However, a strong relationship between P and OM is observed for the levee backslope sediments. Correlation coefficients are provided in Table 6.10.

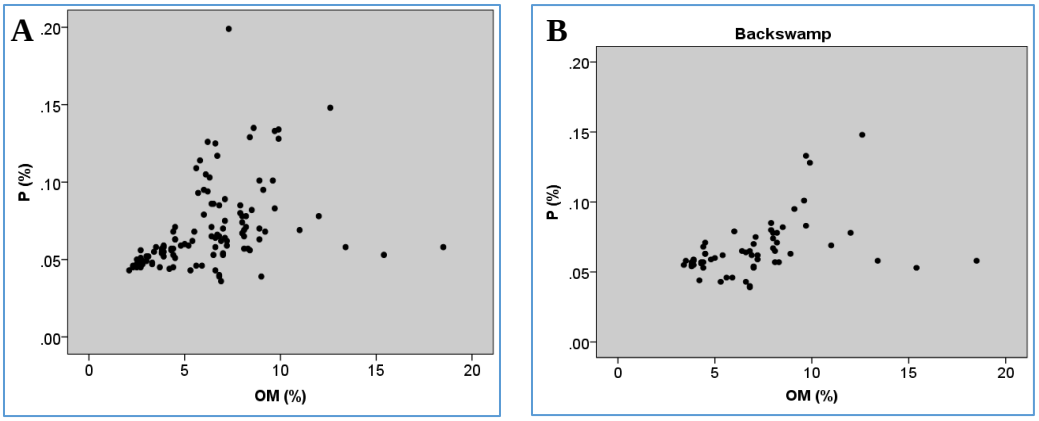

Figure 6.15 Relationship between phosphorus (P) and organic matter (OM) for sediment samples.

(A) Relationship between phosphorus (P) and organic matter (OM) for all sediment samples. (B) Relationship between P and OM for sediment samples from backswamp deposits.

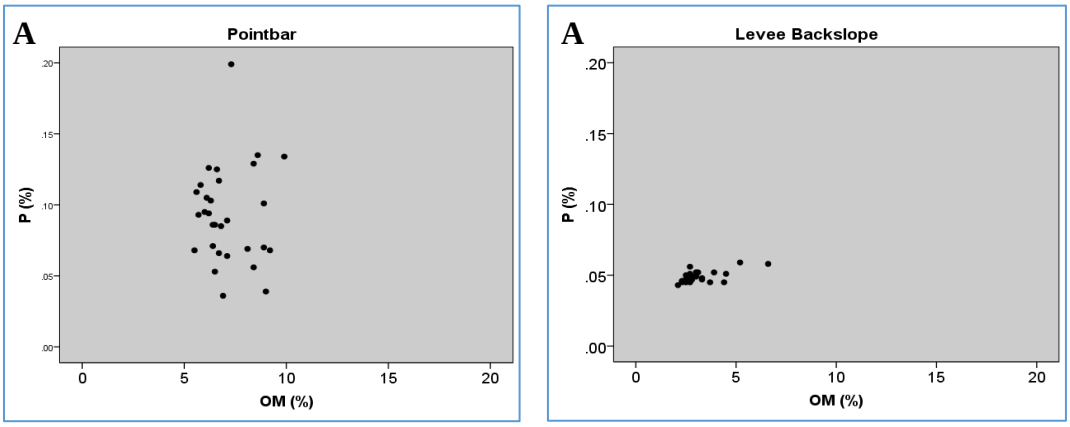

Figure 6.16 Relationship between phosphorus (P) and organic matter (OM) for sediment samples from point-bar deposits and levee backswamp deposits.

Both clay and MS have relatively similar correlation strengths with P, but clay percentage has a positive relationship whereas MS has a negative relationship (Figure 6.17 and figure 6.18). Correlation coefficients for all the parameters are provided in Table 9. Sediment samples from point-bar and levee backslope deposits do not have any

statistical correlation with P and clay percentage. For P and MS, only point-bar deposits have a positive correlation. Table 6.10 summarizes the Pearson correlation values of P and transformed values of clay, OM, and MS.

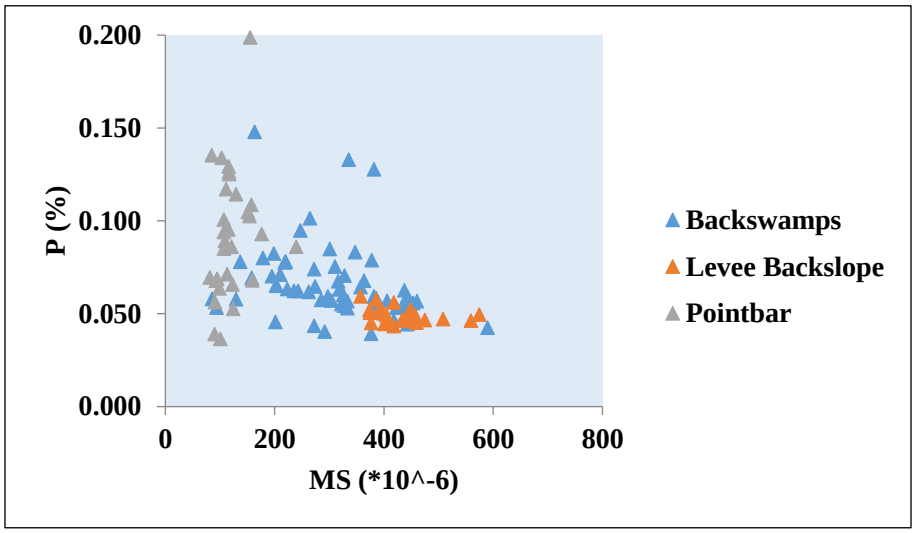

Figure 6.17 Relationship between P and MS for all sediment samples.

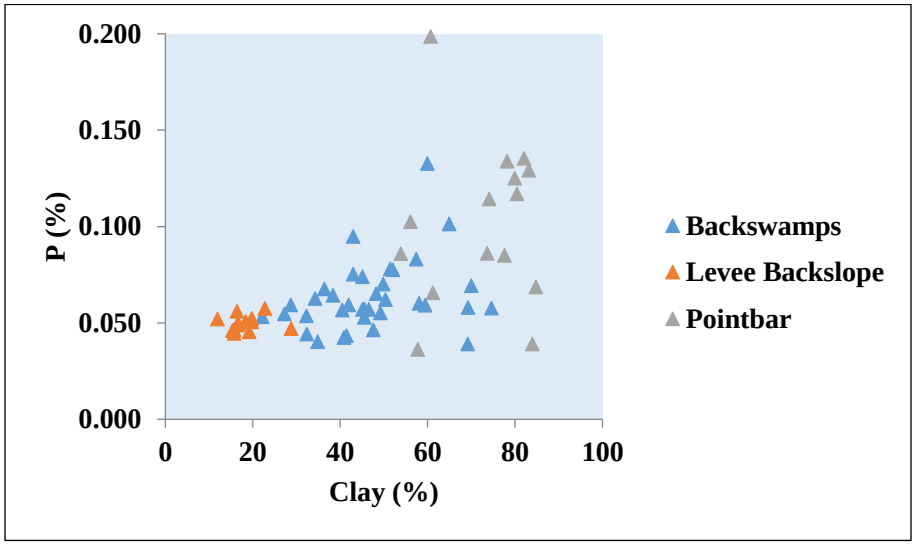

Figure 6.18 Relationship between P and clay percentage for all sediment samples.

Table 6.10

Pearson correlation coefficient values for phosphorus (P), organic matter (OM), clay percentage, and magnetic susceptibility (MS).

	All sediment samples	Backswamp sediments	Point-bar sediments	Levee backslope sediments
P and OM (a)	0.399**	0.397**	-0.020	0.626**
P and $(OM)^2$	0.280**	0.299*	-0.015	0.628**
P and $exp^{(OM)}$	-0.041	-0.057	0.057	0.560**
P and 1/OM	-0.468**	-0.437**	0.028	-0.597**
P and ln (OM)	-0.463**	.444**	-0.025	0.614**
P and Clay (b)	0.553**	0.299	0.057	0.077
P and $(Clay)^2$	0.554**	0.267	0.044	0.053
P and $exp^{(clay)}$	0.012	-0.052	-0.326	-0.210
P and 1/clay	-0.445**	-0.312	-0.082	-0.084
P and ln(clay)	0.514**	-0.315	0.070	0.088
P and MS (c)	-0.519**	-0.259**	0.221	-0.345
P and $(MS)^2$	-0.511**	-0.285*	0.167	-0.318
P and $exp^{(MS)}$	0.000	0.000	-0.038	0.000
P and 1/MS	0.425**	0.125	-0.294	0.397*
P and ln (MS)	-0.489**	-0.205	0.265	-0.371

*- ($P<0.01$), **-($P<0.05$) all the other correlation values are not significant.

(a) Shown in figure 6.15 and 6.16, (b) shown in figure 6.18, (c) shown in figure 6.17.

6.7 CLAY PERCENTAGE, OM, C, N, AND P CONCENTRATIONS

Pointbar sediment sample locations were located at greater distance from the main river channel and levee diposits were placed at the shortest distance from the river channel. Natural levee backslope deposits have a low clay fraction in the top 30 cm of the sediment profile when compared to the other depositional sub-environments (Table 6.11). The upper sediment profiles of point-bar deposits are dominated by clay particles. Backswamp deposits and point-bar deposits have similar amounts of OM within the top

30 cm and levee backslope deposits have relatively low amounts of OM. Both C and N percentages of point-bar deposits are relatively similar but levee backslope deposits have less C and N. Generally, all the sediment samples have high P levels and point-bar deposits have considerably higher values compared to other sub-environments. High MS values are observed for levee backslope deposits and low values are observed in point-bar deposits. C:N (ratio by weight) does not vary much among the depositional sub-environments. Sediment C:N ranged from 10.2–11.8, indicating that sufficient N is available to support microbial activity, with some N available for plant uptake. N:P (ratio by weight) is low for all depositional sub-environments, indicating a high P level in the sediments.

Table 6.11

Clay percentage, OM, C, N, P, MS, C:N (wt:wt), and N:P (wt:wt) for the study area and values for comparison in freshwater depressional and floodplain wetlands of southwestern Georgia (from Craft and Casey, 2008). All values represent the average for top 30 cm.

	This Study			**Craft and Casey (2000)**			
	BSD	**PBD**	**LBD**	**Marsh (D)**	**Savanna (D)**	**Forested (D)**	**Forested (FP)**
Clay (%)	44.8	55.15	19.7	x	x	x	X
OM (%)	8.06	7.05	4.2	x	x	x	X
C (%)	2.27	2.32	1.26	2.5 ± 0.7	2.6 ± 0.9	10 ± 1.3	5.2 ± 1.3
N(%)	0.19	0.22	0.11	0.22 ± 0.05	0.2 ± 0.06	0.72 ± 0.09	0.38 ± 0.08
P (µg/g)	690	1090	540	31 ± 7	116 ± 46	717 ± 92	335 ± 68
MS (*10^{-6})	298	197	391	x	x	x	X
C/N	11.7	10.2	11.8	13 ± 0.8	14 ± 1.9	16 ± 0.3	16 ± 1.1
N/P	2.33	1.72	1.95	228 ± 47	71 ± 39	24 ± 4	26 ± 3

BSD – Backswamp deposit, PBD – Point-bar deposit, LBD – Levee backslope deposit, D – Depressional, FP – Floodplain, x – not available.

Results of a similar study from Craft and Casey (2000) also are provided in Table 6.11. Given the fact that the Mississippi River basin includes a high percentage of agricultural lands associated with nearly continuous applications of fertilizers, insecticides, and pesticides; runoff from these lands should have high concentrations of nutrients such as N and P. However, nutrient concentration results from the present study only reveals high amounts of P whereas the concentrations of N are moderate. Although the study areas are frequently subject to flooding from spring through summer, most of the LMR is not directly connected to its previous floodplain area because of raised artificial levees. Isolation of the river channel could be one reason for less sediment and nutrient deposition in the floodplain in general. However, the study area is not protected by artificial levees and is directly connected to the river channel during flooding. Faster moving floods in the embanked floodplain corridor might efficiently flush sediments and associated nutrients downstream to the Gulf of Mexico. The denitrification process is another possible reason for low (or moderate) N concentrations in the embanked LMR floodplain. Nitrate $(NO_3)^{-1}$, one of the most abundant forms of inorganic N, can be lost to the atmosphere by conversion to gaseous forms of nitrogen through a series of widely occurring biochemical reduction reactions. The study area is subject to periods of alternating drying and wetting because of flood episodes. Anaerobic conditions are favorable to the denitrification process and during flooding a lack of oxygen presents perfect conditions to anaerobic bacterial organisms to carry out the denitrification process that ultimately converts $(NO_3)^{-1}$ into N_2 gas. In addition to denitrification, $(NO_3)^{-1}$ can be lost through leaching because of its high solubility. Because of the negative charge, $(NO_3)^{-1}$ anions are not preferentially adsorbed by negatively charged colloids that

dominate the LMV floodplain deposits. In contrast to $(NO_3)^{-1}$, ammonium $(NH_4)^{+}$ can be easily adsorbed to colloidal surfaces because of its positive charge. This could be a reason for the higher N concentrations in clay-rich point-bar sediments compared to other sub-environments. Craft and Casey (2000) also present low N values for depressional marsh and savanna environments similar to the present study area and denitrification might be the common factor controlling limited N availability. Forested environments high in OM explains the comparatively high N concentrations documented in Craft and Casey (2000).

In contrast to N, P is least soluble (Schonbrunner et al., 2012; Brady and Weil, 2008). Therefore most of the P from agricultural runoff occurs as particulate matter. The reduced solubility of P limits its loss through leaching and increases the P level in the sediments as it accumulates through time. In addition to organic P, primary forms of inorganic P occur as iron- or aluminum-bound inorganic phosphorus. Because of the high positive MS values, it is safe to assume no calcium-bound inorganic phosphorus in the soil. Unlike N, P is not lost by conversion to gaseous forms under anaerobic conditions (Brady and Weil, 2008). However, prolonged anaerobic conditions can reduce Fe^{3+} to Fe^{2+}, thus making the iron-phosphate complex much more soluble. In general accumulations rate of P in drying periods is higher in the studied area compare to the rate of leaching loss during the flooding seasons.

High P concentrations indicate that significant amount of nutrients are supplied to the floodplain by LMR. Denitrification removes N from floodplain and reducing the N from further downstream transport. Significantly high sequestrated P in the soil also indicates that floodplain soils are able to reduce P downstream transportation. Studied

floodplain area is able to act as a sink for both N and P which ultimately helps to control hypoxia in the Gulf region.

6.8 GLOBAL MODEL SIGNIFICANCE FOR C, N, AND P

Statistical results of a global model analysis considering C, N, and P as a response variable and depth, clay, OM and MS as covariates are shown in Table 6.12. The global model for C has a R squared value of 0.641 ($P<0.01$, $N=111$) and it indicates significance for depth, OM, and clay (see appendix for the detailed graphs). There does not appear to have a relationship between C and MS in the global model. OM has the largest effect on carbon (0.54) and next strongest variable affecting C is clay (0082). The effect of OM is almost an order of magnitude larger than the clay (0.082). Three reduced models for C (depth and clay, depth and OM, depth and MS) were analyzed and out of those models C with depth and OM shows the strongest corrected model effect size of 0.631 (see appendix).

The global model for N has a R squared value of 0.638 ($P<0.01$, $N=111$). Similar to C, OM has the largest effect (0.444) on N and depth also has an effect of 0.181. Clay and MS do not appear to have significant relationships with N in the global model. Three reduced model were considered for N similar to C. Out of those models N with depth and OM appear to have the strongest corrected model effect size of (0.646) (see appendix).

The global model for P has the lowest R squared value (0.367) compared to C and N. In contrast to C and N, depth (0.056) and clay percentage (0.088) has the significant effect on P. OM and MS does not appear to have a significance correlation with P in the global model. Out of three reduced models P with depth and clay shows the highest corrected model effect on P (0.318) (see appendix).

Table 6.12

Subjects effects of global models for C, N and P.

Global model	N	df	F	Sig.	Partial Eta Squared
C*	111	4	47.312	0	0.641
N*	111	4	46.723	0	0.638
P*	64	4	8.559	0	0.367

* - considering depth, clay, OM and MS as covariates.

CHAPTER VII – CONCLUSION

This study reveals that all the measured sediment characteristics such as particle size of the sediments, OM content, MS of the sediments, C, N and P concentrations vary with the depth. Except for few localized incidents all the studied sediment cores show high OM, C and N concentration at the top soil and gradually decrease with depth and become relatively constant at no more than 25 cm depth. All the sediment analysis from the study area reveals high MS associated with the silt and sand size fraction. Compare to C and N, P does not vary much with depth. Comparison between three sub-environments for the top 30 cm reveals that sediment characteristics are changing based on the environment type. Comparatively point-bar sediments have high clay fraction and levee backslope sediments are rich in silt and sand size fraction. Backswamp sediments have moderate clay percentage. Average OM, C and N concentrations are relatively similar at the topsoil but levee backslope sediments have lower OM, C and P concentrations. Point-bar sediments have significantly higher P concentrations compare to other environments. Levee backslope sediments appear to have the highest MS content because of the low clay percentage.

According to the C, N, and P concentrations, the study area has moderate C, N and significantly high concentrations of P compared to other regions. C and N are mainly originated from OM of the soil and P has higher inorganic P content. Depth and OM are the main factors governing the C and N concentrations. MS and clay appear to have less significance in determining C and N concentrations. Depth and clay fraction is more important in determining the P concentrations in the study area while OM and MS appear to have less significance.

Future consideration for this research would require the need of higher number of sediment core samples equally distributed among the environments types to generalize the results obtained for three different sub-environments. Results of this study show the ability of a natural floodplain to reduce further downstream transportation of nutrients. Having a natural floodplain/wetland in between agricultural lands and river channel is important in naturally reducing the nutrients level that are delivering in to the Gulf region and ultimately causing the eutrophication. In addition to spatial changes it is also important to analyze the temporal sedimentary depositional changes in order to model how much volume of nutrients are sequestrated in the LMAV without being contribute to the hypoxia in the Gulf of Mexico. Quantifying the ability of sequestrating nutrients will help in environmental management perspective.

APPENDIX A – SEDIMENT CORE RESULTS

Table A.1

Results for the sediment core MS.SC01

Depth (cm)	Clay (%)	Silt (%)	Sand (%)	N (%)	C (%)	P (%)	OM (%)	MS LF (e-6)	MS HF (e-6)
0	57.4	41.4	1.1	0.31	3.84	0.083	9.7	347.8	327.7
10	46.6	39.2	14.2	0.16	1.96	0.057	8.1	406.4	385.9
20	32.3	36	31.7	0.09	1.25	0.054	7.0	433.8	412.7
30	22.2	41.9	35.9	0.08	1.23	0.053	7.0	422.9	408.4
40	47.6	37.2	15.2	0.05	0.81	0.046	5.6	418.6	400.5
50	40.9	53	6.1	0.05	0.69	0.043	5.3	589.9	574.0
60	69.2	29.5	1.4	0.05	0.7	0.039	6.8	376.9	356.1
70	34.9	63.8	1.3	0.08	0.97	0.040	6.8	291.7	279.8
80	41.5	58.2	0.3	0.04	0.6	0.043	6.6	272.8	264.8
90	59.5	40.1	0.4	0.07	0.89	0.059	7.2	297.9	283.7
100	33.8	65.6	0.6	0.07	0.93	x	6.6	242.0	231.8
110	46.6	52.9	0.5	0.07	0.89	x	5.9	282.4	272.5
120	45	54.8	0.2	0.07	0.89	x	6.3	344.6	319.4
130	32.7	67	0.3	0.09	1.08	x	6.6	355.6	333.9
140	52.8	46.9	0.3	0.08	0.92	x	6.4	309.1	292.0
150	53.7	46.1	0.2	0.07	0.81	x	6.1	282.4	267.6
160	47.6	52.1	0.2	0.08	0.84	x	5.9	245.4	236.1

x – Not measured , LF- Low frequency, HF- High frequency

Table A.2

Results for the sediment core MS.SC02

Depth (cm)	Clay (%)	Silt (%)	Sand (%)	N (%)	C (%)	P (%)	OM (%)	MS LF (e-6)	MS HF (e-6)
0	46	53	0.4	0.22	2.47	x	12.6	273.8	257.6
5	x	x	x	0.2	2.4	x	9	271.8	267.5
10	43.5	54.7	1.9	0.18	2.09	x	10.6	297.3	288.7
15	x	x	x	0.18	2	x	9.1	392.8	345.5
20	33.8	63.5	2.7	0.15	1.77	x	8.5	327.0	316.4
25	x	x	x	0.09	1.05	x	7	443.4	423.2
30	29.3	61.8	8.9	0.1	1.23	x	5.5	368.3	337.6
35	x	x	x	0.09	1.05	x	5.4	426.9	405.0
40	29.7	69.5	0.7	0.09	1.12	x	5.8	368.0	349.2
45	x	x	x	0.08	1.08	x	5.3	388.3	394.8
50	31.8	65.6	2.6	0.1	1.32	x	5.2	346.2	363.7

55	x	x	x	0.07	0.97	x	4.7	472.2	454.3
60	32.3	61.7	5.9	0.08	1.08	x	5	348.5	344.9
65	x	x	x	0.09	1.13	x	4.7	317.1	307.9
70	37.9	61	1.1	0.1	1.08	x	5.6	278.7	276.1
75	x	x	x	0.12	1.21	x	7.2	317.7	296.6
80	45	53.9	1	0.12	1.25	x	7.3	360.4	341.3
85	x	x	x	0.09	0.87	x	6.4	291.6	277.1
90	42.4	56.8	0.8	0.1	1.06	x	7.2	275.1	260.5
95	x	x	x	0.07	0.79	x	6	291.7	278.1
100	43	56.5	0.6	0.08	0.9	x	6.2	348.2	328.0
105	x	x	x	0.07	0.81	x	6	349.2	332.6
110	40.4	59.3	0.4	0.08	0.86	x	5.6	291.3	296.2
115	x	x	x	0.09	0.95	x	6.8	339.6	315.5
120	43	56.9	0.2	0.08	0.86	x	6.2	266.9	241.4
125	x	x	x	x	x	x	6.2	318.8	305.8
130	49.2	50.5	0.3	x	x	x	6.3	238.4	225.9
135	x	x	x	x	x	x	6.4	328.0	288.3
140	44	55.7	0.3	x	x	x	6.5	215.9	207.6
145	x	x	x	x	x	x	5.8	275.8	261.2
150	47.1	52.6	0.3	x	x	x	6	271.5	238.8
155	x	x	x	x	x	x	6.4	192.1	182.2
160	44.5	55.2	0.3	x	x	x	5.7	197.2	192.1
165	x	x	x	x	x	x	6.4	201.4	190.8
170	58.8	40.3	0.8	x	x	x	6.7	120.7	120.0
175	x	x	x	x	x	x	6.8	137.9	136.6
180	61.4	38	0.6	x	x	x	7.7	122.3	115.7
185	x	x	x	x	x	x	7.4	115.1	120.0
190	69.1	30.3	0.6	x	x	x	10.1	124.0	112.1
195	x	x	x	x	x	x	8.6	84.3	85.0
200	80.3	19.4	0.3	x	x	x	9.2	110.1	109.1
205	x	x	x	x	x	x	8.9	113.1	115.4
210	79.4	20	0.5	x	x	x	8.5	110.5	114.8
215	x	x	x	x	x	x	8.9	116.7	114.7
220	77.3	21.5	1.2	x	x	x	7.4	111.7	117.4
225	x	x	x	x	x	x	7.3	91.9	95.5
230	x	x	x	x	x	x	6.7	121.7	138.2
235	x	x	x	x	x	x	7	122.4	117.7
240	x	x	x	x	x	x	6.4	130.2	120.7
245	x	x	x	x	x	x	6.9	103.5	111.5

x – Not measured , LF- Low frequency, HF- High frequency

Table A.3

Results for the sediment core MS.SC03

Depth (cm)	Clay (%)	Silt (%)	Sand (%)	N (%)	C (%)	P (%)	OM (%)	MS LF (e^{-6})	MS HF (e^{-6})
0	43	55.7	1.3	0.23	2.32	0.09	9.1	247.6	238.1
5	x	x	x	0.2	2.11	0.06	8.9	223.2	219.2
10	45.6	53.9	0.5	0.17	1.95	0.06	8.3	285.3	276.1
15	x	x	x	0.13	1.49	0.07	8.0	316.4	294.7
20	45.1	53.9	1	0.13	1.49	0.07	8.0	272.8	265.9
25	x	x	x	0.1	1.07	0.06	6.4	274.5	265.2
30	50.4	49.2	0.4	0.1	1.08	0.06	6.9	243.4	235.4
35	x	x	x	0.11	1.25	0.07	8.1	204.0	201.7
40	51.5	47.3	1.1	0.11	1.15	0.08	8.0	220.2	215.9
45	x	x	x	0.1	1.1	0.07	8.2	210.3	204.7
50	52.1	46.7	1.2	0.11	1.17	0.08	8.2	218.5	213.9
55	x	x	x	0.1	1.01	0.06	7.2	235.7	211.9
60	48.3	51.2	0.5	0.09	0.95	0.07	6.8	202.7	206.3
65	x	x	x	0.09	0.97	0.08	8.5	199.1	192.7
70	49.9	49.1	1.1	0.1	1.04	0.07	7.0	195.4	196.4
75	x	x	x	0.1	1.08	0.08	7.9	178.8	178.7
80	65	32.8	2.1	0.13	1.27	0.10	9.6	264.8	253.3
85	x	x	x	0.15	1.65	0.13	9.9	381.9	352.8
90	60	37.4	2.6	0.17	1.95	0.13	9.7	336.0	321.7
95	x	x	x	0.22	3.13	0.15	12.6	163.7	160.7
100	70	28.3	1.7	0.22	3.06	0.07	11.0	158.4	160.1
105	x	x	x	0.19	2.83	0.08	12.0	137.2	133.6
110	74.6	24.6	0.9	0.21	2.76	0.06	13.4	129.6	130.6
115	x	x	x	0.28	6.34	0.05	15.4	94.3	88.6
120	69.3	28.3	2.4	0.26	4.89	0.06	18.5	85.7	80.7
125	x	x	x	x	x	x	18.4	81.4	81.8
130	70.7	28.1	1.3	x	x	x	16.4	87.3	85.3
135	x	x	x	x	x	x	15.0	101.5	100.5
140	70	28.4	1.7	x	x	x	16.9	88.2	89.0
145	x	x	x	x	x	x	20.0	84.7	84.4

x – Not measured , LF- Low frequency, HF- High frequency

Table A.4

Results for the sediment core MS.SC04

Depth (cm)	Clay (%)	Silt (%)	Sand (%)	N (%)	C (%)	P (%)	OM (%)	MS LF (e^{-6})	MS HF (e^{-6})
0	43	56.6	0.4	0.16	1.97	0.08	7.1	310.8	298.9
5	x	x	x	0.18	2.04	0.08	7.9	301.5	284.3
10	38.4	60.4	1.2	0.15	1.7	0.06	6.6	357.5	338.3
15	x	x	x	0.14	1.52	0.08	6.0	378.3	361.7
20	36.4	51.3	12.3	0.13	1.36	0.07	4.4	363.8	350.8
25	x	x	x	0.09	0.98	0.06	3.5	386.2	373.9
30	27.3	44.6	28.2	0.08	1	0.05	3.8	388.1	379.2
35	x	x	x	0.07	0.89	0.06	3.4	447.0	424.5
40	32.4	61.7	5.9	0.07	0.96	0.04	4.2	443.1	421.3
45	x	x	x	0.08	1.02	0.06	3.8	460.6	443.1
50	28.7	70.1	1.2	0.08	1.05	0.06	3.9	442.7	422.3
55	x	x	x	0.09	1.11	0.06	4.3	453.3	434.5
60	34.3	64.5	1.2	0.09	1.11	0.06	4.5	437.5	422.6
65	x	x	x	0.1	1.2	0.07	4.5	328.3	317.8
70	42	57.4	0.7	0.09	0.96	0.06	4.8	381.9	379.0
75	x	x	x	0.08	0.91	0.06	4.5	318.8	322.0
80	58.1	41.5	0.4	0.1	1.08	0.06	5.0	326.0	310.5
85	x	x	x	0.07	0.84	0.05	5.9	201.7	182.9
90	49.2	50.3	0.5	0.07	0.87	0.06	3.9	322.1	311.5
95	x	x	x	0.1	1.03	0.06	5.4	262.5	239.8
100	45.1	54.3	0.6	0.07	0.89	0.06	4.4	304.2	295.6
105	x	x	x	0.05	0.79	0.05	3.8	327.3	289.7
110	45.6	54.2	0.2	0.07	0.88	0.05	4.4	333.7	319.4
115	x	x	x	0.05	0.82	0.06	3.9	383.9	365.0
120	40.5	59.3	0.3	0.07	0.79	0.06	4.3	333.3	321.7
125	x	x	x	x	x	x	4.9	364.0	330.7
130	45.1	54.4	0.5	x	x	x	4.3	352.1	339.0
135	x	x	x	x	x	x	5.1	288.4	273.9
140	47.2	52.5	0.3	x	x	x	4.4	373.0	352.8
145	x	x	x	x	x	x	4.8	330.3	311.2

x – Not measured , LF- Low frequency, HF- High frequency

Table A.5

Results for the sediment core MS.CAT05

Depth (cm)	Clay (%)	Silt (%)	Sand (%)	N (%)	C (%)	P (%)	OM (%)	MS LF (e^{-6})	MS HF (e^{-6})
0	53.4	43.7	3	0.67	10.79	x	16.4	140.9	136.5
5	x	x	x	0.42	5.43	x	10.1	129.7	129.2
10	55.4	44.4	0.2	0.21	2.39	x	6.5	147.1	147.5

15	x	x	x	0.12	1.2	x	5.9	145.8	144.5
20	52.3	47.3	0.4	0.13	1.43	x	6.1	147.8	144.8
25	x	x	x	0.1	0.98	x	5.7	136.9	134.3
30	43	56.7	0.3	0.09	0.92	x	5.2	129.3	133.2
35	x	x	x	0.08	0.72	x	4.9	142.5	142.5
40	35.9	63.7	0.4	0.07	0.61	x	5.0	138.9	134.3
45	x	x	x	0.04	0.33	x	3.7	105.5	114.4
50	38.4	61.3	0.3	0.06	0.52	x	4.6	122.3	119.0
55	x	x	x	0.08	0.7	x	4.3	110.3	105.8
60	29.8	69.7	0.5	0.04	0.37	x	3.9	112.8	112.1
65	x	x	x	0.05	0.42	x	4.3	118.1	117.1
70	57.1	42.3	0.6	x	x	x	x	x	x
75	x	x	x	0.09	0.88	x	5.3	97.3	96.3
80	69.3	29.8	0.9	0.11	1.04	x	6.3	127.3	125.6
85	x	x	x	0.1	0.92	x	6.4	118.1	118.1
90	82.6	17.1	0.3	0.09	0.78	x	6.2	121.7	120.7
95	x	x	x	0.1	0.8	x	6.4	112.8	111.1
100	85.8	14	0.2	0.1	0.81	x	7.5	109.4	109.1
105	x	x	x	0.1	0.9	x	6.3	116.7	115.1
110	91.8	7.9	0.3	0.09	1.52	x	6.6	110.5	111.5
115	x	x	x	0.1	1.39	x	6.6	128.6	126.7
120	86.3	13.3	0.4	0.1	1.21	x	7.2	130.9	133.9
125	x	x	x	0.11	1.26	x	8.3	141.2	137.2
130	82	17.3	0.7	x	x	x	7.5	127.7	126.7
135	x	x	x	x	x	x	7.3	123.3	121.3
140	82.8	16.9	0.2	x	x	x	7.5	130.3	132.6
145	x	x	x	x	x	x	7.8	125.3	125.8

x – Not measured , LF- Low frequency, HF- High frequency

Table A.6

Results for the sediment core MS.CAT06

Depth (cm)	**Clay (%)**	**Silt (%)**	**Sand (%)**	**N (%)**	**C (%)**	**P (%)**	**OM (%)**	**MS LF (e-6)**	**MS HF (e-6)**
0	51.9	45.2	2.9	0.59	7.42	x	12.5	165.0	164.0
5	x	x	x	0.34	3.71	x	10.4	141.8	137.9
10	53.9	45	1.1	0.14	1.38	x	6.1	303.9	291.3
15	x	x	x	0.14	1.44	x	6.0	266.2	257.2
20	54.3	44.6	1.1	0.13	1.45	x	6.5	240.1	228.5
25	x	x	x	0.12	1.24	x	5.8	209.0	214.9
30	54.4	44.9	0.7	0.09	0.98	x	5.5	253.6	241.0
35	x	x	x	0.10	1	x	5.8	260.5	246.0

40	60.3	39.3	0.4	0.11	1.11	x	5.5	302.5	281.0
45	x	x	x	0.10	1.07	x	5.7	229.1	218.3
50	57	42.6	0.4	0.10	1.05	x	5.3	240.1	225.1
55	x	x	x	0.10	1	x	5.9	290.0	274.8
60	58.2	41.4	0.4	0.10	1	x	5.9	222.2	209.3
65	x	x	x	0.10	1	x	5.6	170.3	165.3
70	58.6	41.1	0.3	0.09	0.92	x	5.0	204.7	194.1
75	x	x	x	0.10	1.01	x	4.7	223.5	216.6
80	58.6	41	0.4	0.10	0.97	x	5.0	175.6	176.9
85	x	x	x	0.09	0.97	x	4.9	233.8	225.9
90	62	37.3	0.7	0.11	0.96	x	5.0	184.5	186.2
95	x	x	x	0.10	0.87	x	5.2	161.4	161.0
100	62.9	36.1	1	0.11	1.03	x	6.4	148.5	147.2
105	x	x	x	0.10	0.9	x	5.6	135.9	137.2
110	60.3	39	0.7	0.11	0.9	x	5.1	147.8	154.4
115	x	x	x	0.10	0.78	x	5.0	199.4	194.1
120	52.9	46.5	0.6	0.09	0.76	x	5.3	173.5	171.3
125	x	x	x	0.11	0.86	x	6.0	117.1	115.7
130	78.1	21.7	0.2	0.14	1.15	x	6.0	107.5	108.8
135	x	x	x	x	x	x	5.9	106.2	107.5
140	75.4	24.1	0.5	x	x	x	5.6	105.5	106.8
145	x	x	x	x	x	x	5.4	106.8	114.7

x – Not measured , LF- Low frequency, HF- High frequency

Table A.7

Results for the sediment core MS.CAT07.

Depth (cm)	**Clay (%)**	**Silt (%)**	**Sand (%)**	**N (%)**	**C (%)**	**P (%)**	**OM (%)**	**MS LF (e^{-6})**	**MS HF (e^{-6})**
0	22.8	64.4	12.8	0.18	2.27	0.058	6.6	385.9	378.3
5	x	x	x	0.14	1.65	0.059	5.2	357.5	351.5
10	19.8	59.3	21	0.13	1.46	0.051	4.5	375.0	366.3
15	x	x	x	0.09	1	0.052	3.9	374.0	375.0
20	16.4	41.2	42.5	0.06	0.67	0.056	2.7	418.6	413.6
25	x	x	x	0.04	0.52	0.046	2.6	436.1	431.1
30	12	40.5	47.5	0.05	0.63	0.052	3.1	448.7	441.1
35	x	x	x	0.05	0.75	0.049	3.0	405.0	401.4
40	18.4	61.7	19.9	0.04	0.54	0.051	2.7	393.8	385.9
45	x	x	x	0.05	0.64	0.050	2.5	399.4	392.5
50	19.8	52.6	27.6	0.05	0.63	0.052	3.0	393.5	382.9
55	x	x	x	0.04	0.6	0.045	4.4	376.9	365.0
60	15.8	37.8	46.5	0.03	0.49	0.045	2.7	410.0	402.1

65	x	x	x	0.02	0.41	0.043	2.1	418.6	412.3
70	19.2	46.3	34.6	0.02	0.52	0.045	3.7	403.4	397.3
75	x	x	x	0.02	0.48	0.047	2.8	434.5	427.2
80	28.8	56.8	14.4	0.02	0.46	0.047	3.3	440.1	432.5
85	x	x	x	0.03	0.57	0.045	2.5	401.4	393.5
90	15.8	54.2	30.1	0.03	0.57	0.047	2.5	475.5	464.6
95	x	x	x	0.03	0.55	0.047	2.5	508.5	498.3
100	15.4	47.3	37.4	0.03	0.55	0.046	2.3	559.4	551.2
105	x	x	x	0.03	0.59	0.045	2.3	460.3	445.4
110	16.4	48.4	35.2	0.03	0.55	0.049	2.8	457.6	444.7
115	x	x	x	0.03	0.57	0.048	3.3	443.1	434.5
120	16.8	45.5	37.8	0.03	0.5	0.049	2.7	574.6	564.5
125	x	x	x	x	x	x	2.2	756.6	750.3
130	18.8	47.4	33.8	x	x	x	3.3	528.7	521.4
135	x	x	x	x	x	x	2.9	462.3	451.7
140	23.8	60.3	15.9	x	x	x	3.6	381.6	373.6
145	x	x	x	x	x	x	4.5	304.8	297.6

x – Not measured , LF- Low frequency, HF- High frequency

Table A.8

Results for the sediment core MS.SC 08.

Depth (cm)	**Clay (%)**	**Silt (%)**	**Sand (%)**	**N (%)**	**C (%)**	**P (%)**	**OM (%)**	**MS LF (e^{-6})**	**MS HF (e^{-6})**
0	60.7	37.3	2	0.44	4.09	0.199	7.3	155.4	152.1
5	x	x	x	0.22	2.03	0.105	6.1	151.2	147.5
10	56.1	40.4	3.5	0.14	1.33	0.103	6.3	154.4	148.8
15	x	x	x	0.13	1.3	0.093	5.7	176.6	173.3
20	53.9	44.2	2	0.13	1.26	0.086	6.5	240.0	244.0
25	x	x	x	0.12	1.19	0.068	5.5	159.4	156.7
30	61.2	37.6	1.2	0.12	1.3	0.066	6.7	123.3	130.0
35	x	x	x	0.13	1.29	0.053	6.5	124.4	123.0
40	57.8	41.6	0.7	0.15	1.64	0.036	6.9	100.9	93.9
45	x	x	x	0.13	1.18	0.089	7.1	109.1	108.1
50	77.6	21.1	1.2	0.14	1.25	0.085	6.8	107.5	110.1
55	x	x	x	0.15	1.26	0.056	8.4	91.0	94.2
60	82.1	17.4	0.4	0.18	1.72	0.135	8.6	85.0	86.9
65	x	x	x	0.22	2.2	0.070	8.9	81.4	84.8
70	83.2	15.7	1.1	0.19	1.78	0.129	8.4	116.0	115.4
75	x	x	x	0.24	2.53	0.101	8.9	107.4	108.8
80	78.2	19.5	2.3	0.26	2.8	0.134	9.9	103.6	92.1
85	x	x	x	0.23	2.93	0.068	9.2	92.8	92.2

90	84.8	14.6	0.5	0.18	1.82	0.069	8.1	94.9	95.9
95	x	x	x	0.18	1.98	0.064	7.1	99.2	101.5
100	84	15.4	0.6	0.13	1.4	0.039	9.0	90.3	91.9
105	x	x	x	0.11	1	0.071	6.4	113.5	102.2
110	80.5	18.2	1.3	0.11	0.93	0.117	6.7	111.4	111.8
115	x	x	x	0.12	1.13	0.094	6.2	107.4	100.5
120	80	18.8	1.2	0.1	0.94	0.125	6.6	116.8	117.1
125	x	x	x	0.09	0.8	0.12632	6.2	116.7	117.4
130	73.7	25.1	1.2	0.08	0.7	0.086099	6.4	121.3	121.0
135	x	x	x	0.07	0.63	0.095292	6.0	115.8	116.4
140	74.1	25.6	0.3	0.09	0.83	0.114394	5.8	129.6	125.7
145	x	x	x	x	x	0.108635	5.6	157.5	154.2

x – Not measured , LF- Low frequency, HF- High frequency

APPENDIX B – GLOBAL MODEL ANALYSIS RESULTS

Table B.1

Global model analysis between C as response variable, and depth, clay, OM and MS as variables.

Source	Type III Sum of Squares	df	Mean Square	F	Sig.	Partial Eta Squared
Corrected Model	119.025[a]	4	29.756	47.312	0	0.641
Intercept	0.006	1	0.006	0.01	0.922	0
Depth	5.984	1	5.984	9.515	0.003	0.082
OM	78.166	1	78.166	124.284	0	0.54
Clay	2.065	1	2.065	3.283	0.073	0.03
MS	0.355	1	0.355	0.565	0.454	0.005
Error	66.667	106	0.629			
Total	399.543	111				
Corrected Total	185.691	110				

Dependent Variable: Nitrogen

a - R Squared = .638 (Adjusted R Squared = .624)

Table B.2

Global model analysis between P as response variable, and depth, clay, OM and MS as variables.

Source	Type III Sum of Squares	df	Mean Square	F	Sig.	Partial Eta Squared
Corrected Model	.021[a]	4	0.005	8.559	0	0.367
Intercept	0.005	1	0.005	7.282	0.009	0.11
Depth	0.002	1	0.002	3.481	0.067	0.056
OM	0.001	1	0.001	1.235	0.271	0.021
Clay	0.004	1	0.004	5.668	0.021	0.088
MS	0.001	1	0.001	1.516	0.223	0.025
Error	0.037	59	0.001			
Total	0.369	64				
Corrected Total	0.058	63				

Dependent Variable: P, a - R Squared = .367

Table B.3

Model analysis between C as the response variable and depth and OM as variables

Source	Type III Sum of Squares	df	Mean Square	F	Sig.	Partial Eta Squared
Corrected Model	165.902[a]	2	82.951	166.739	0	0.631
Intercept	3.372	1	3.372	6.779	0.01	0.034
Depth	12.707	1	12.707	25.542	0	0.116
OM	146.638	1	146.638	294.755	0	0.602
Error	97.011	195	0.497			
Total	620.911	198				
Corrected Total	262.913	197				

Dependent Variable: Carbon, a. R Squared = .631 (Adjusted R Squared = .627)

Table B.4

Model analysis between C as the response variable and depth and clay as variables.

Source	Type III Sum of Squares	df	Mean Square	F	Sig.	Partial Eta Squared
Corrected Model	38.598[a]	2	19.299	14.17	0	0.208
Intercept	18.303	1	18.303	13.439	0	0.111
Depth	31.315	1	31.315	22.992	0	0.176
Clay	17.808	1	17.808	13.075	0	0.108
Error	147.094	108	1.362			
Total	399.543	111				
Corrected Total	185.691	110				

Dependent Variable: Carbon, a. R Squared = .208 (Adjusted R Squared = .193)

Table B.5

Model analysis between C as the response variable and depth and MS as variables.

Source	Type III Sum of Squares	df	Mean Square	F	Sig.	Partial Eta Squared
Corrected Model	46.485[a]	2	23.242	20.941	0	0.177
Intercept	157.283	1	157.283	141.711	0	0.421
Depth	26.93	1	26.93	24.264	0	0.111
MS	27.22	1	27.22	24.525	0	0.112
Error	216.428	195	1.11			
Total	620.911	198				
Corrected Total	262.913	197				

Dependent Variable: Carbon, a. R Squared = .177 (Adjusted R Squared = .168)

Table B.6

Model analysis between N as the response variable and depth and OM as variables

Source	Type III Sum of Squares	df	Mean Square	F	Sig.	Partial Eta Squared
Corrected Model	.869[a]	2	0.434	178.241	0	0.646
Intercept	0	1	0	0.068	0.794	0
Depth	0.113	1	0.113	46.198	0	0.192
OM	0.714	1	0.714	293.019	0	0.6
Error	0.475	195	0.002			
Total	4.032	198				
Corrected Total	1.344	197				

Dependent Variable: Nitrogen , a. R Squared = .646 (Adjusted R Squared = .643)

Table B.7

Model analysis between N as the response variable and depth and clay as variables.

Source	Type III Sum of Squares	df	Mean Square	F	Sig.	Partial Eta Squared
Corrected Model	.315[a]	2	0.157	26.488	0	0.329
Intercept	0.097	1	0.097	16.258	0	0.131
Depth	0.228	1	0.228	38.355	0	0.262
Clay	0.178	1	0.178	29.928	0	0.217
Error	0.642	108	0.006			
Total	2.539	111				
Corrected Total	0.957	110				

Dependent Variable: Nitrogen, a. R Squared = .329 (Adjusted R Squared = .317)

Table B.8

Model analysis between N as the response variable and depth and MS as variables.

Source	Type III Sum of Squares	df	Mean Square	F	Sig.	Partial Eta Squared
Corrected Model	.427[a]	2	0.214	45.442	0	0.318
Intercept	1.319	1	1.319	280.576	0	0.59
Depth	0.225	1	0.225	47.789	0	0.197
MS	0.273	1	0.273	57.985	0	0.229
Error	0.917	195	0.005			
Total	4.032	198				
Corrected Total	1.344	197				

Dependent Variable: Nitrogen, a. R Squared = .318 (Adjusted R Squared = .311)

Table B.9

Model analysis between P as the response variable and depth and OM as variables.

Source	Type III Sum of Squares	df	Mean Square	F	Sig.	Partial Eta Squared
Corrected Model	.014[a]	2	0.007	10.733	0	0.161
Intercept	0.027	1	0.027	41.698	0	0.271
Depth	0	1	0	0.2	0.655	0.002
OM	0.013	1	0.013	20.867	0	0.157
Error	0.072	112	0.001			
Total	0.643	115				
Corrected Total	0.086	114				

Dependent Variable: P, a. R Squared = .161 (Adjusted R Squared = .146)

Table B.10

Model analysis between P as the response variable and depth and clay as variables.

Source	Type III Sum of Squares	df	Mean Square	F	Sig.	Partial Eta Squared
Corrected Model	.020[a]	2	0.01	15.829	0	0.342
Intercept	0.013	1	0.013	20.434	0	0.251
Depth	0.002	1	0.002	3.365	0.071	0.052
Clay	0.02	1	0.02	31.646	0	0.342
Error	0.038	61	0.001			
Total	0.369	64				
Corrected Total	0.058	63				

Dependent Variable: P , a. R Squared = .342 (Adjusted R Squared = .320)

Table B.11

Model analysis between P as the response variable and depth and MS as variables.

Source	Type III Sum of Squares	df	Mean Square	F	Sig.	Partial Eta Squared
Corrected Model	.023[a]	2	0.012	20.756	0	0.27
Intercept	0.121	1	0.121	215.369	0	0.658
Depth	0	1	0	0.239	0.626	0.002
MS	0.023	1	0.023	40.824	0	0.267
Error	0.063	112	0.001			
Total	0.643	115				
Corrected Total	0.086	114				

Dependent Variable: P , a. R Squared = .270 (Adjusted R Squared = .257)

REFERENCES

Acreman, M., & Holden, J. (2013). How wetlands affect floods. Wetlands, 33(5), 773-786.

Aslan, A., and Autin, W., 1998, Holocene flood-plain soil formation in the southern lower Mississippi Valley: Implications for interpreting alluvial paleosols of the Mississippi River: Significance for the interpretation of alluvial paleosols: Geological Science of America Bulletin, v. 110; no. 4; p. 433–449.

Aslan, A., and Autin, W.J., 1999, Evolution of the Holocene Mississippi River floodplain, Ferriday, Louisiana; insights on the origin of fine-grained floodplains: Journal of Sedimentary Research, v. 69, p. 800–815.

Autin, W. J., Burns, S.F, Miler, B.J, Saucier, R.T, and Snead, J. I., (1991) Quaternary geology of the lower Mississippi Valley. In: Quaternary Nonglacial Geology : Conteerminous (R.B Morrison Ed.) USGA, Boulder, CO, pp 547-582.

Bernard, H.A and Major C.F Jr., 1963, Recent meander belt deposits of the Brazos River: an alluvial sand model, The American Association of Petroleum Geologist, 47, p350.

Baker, R. G., Gonzalez, L. A., Raymo, M., Bettis, E. A., Reagan, M. K., & Dorale, J. A. (1998). Comparison of multiple proxy records of Holocene environments in the midwestern United States. Geology, 26(12), 1131-1134.

Baker, R., 2000, Holocene environments reconstructed from plant macrofossils in stream deposits from southeastern Nebraska, USA: The Holocene, v. 10, p. 357–365.

Balsam, W.L., and Beeson, J.P., 2003, Sea-floor sediment distribution in the Gulf of Mexico: Deep Sea Research Part I: Oceanographic Research Papers, v. 50, p. 1421–1444, doi: 10.1016/j.dsr.2003.06.001.

Bannister, J. M., Herbert, E. R., & Craft, C. B. (2015). Spatial variability in sedimentation, carbon sequestration, and nutrient accumulation in an alluvial floodplain Forest. In The Role of Natural and Constructed Wetlands in Nutrient Cycling and Retention on the Landscape (pp. 41-55). Springer International Publishing.

Battaglia, L. L., Minchin, P. R., & Pritchett, D. W. (2002). Sixteen years of old-field succession and reestablishment of a bottomland hardwood forest in the Lower Mississippi Alluvial Valley. Wetlands, 22(1), 1-17.

Blum, M.D, Guccione, M.J, Wysocki, D.A, Robnett, P.C, and Ruteldge, E.M., (2000), Late pleistocene evolution of the lower Misssissippi River valley, Geological society of America bulletin, 112(2), p: 221-235.

Brady, N.C and Weil, R.R., 2008, Elements of the nature and the properties of soils, 3rd ed.

Cazanacli, D., & Smith, N. D. (1998). A study of morphology and texture of natural levees—Cumberland Marshes, Saskatchewan, Canada. Geomorphology, 25(1), 43-55.

Collinson, J. D. (1996). Alluvial sediments. Sedimentary Environments: Process, Facies and Stratigraphy, 37-82.

Craft, C. B., & Casey, W. P. (2000). Sediment and nutrient accumulation in floodplain and depressional freshwater wetlands of Georgia, USA. Wetlands, 20(2), 323-332.

Dean, W.E., 1997, Rates, timing, and cyclicity of Holocene eolian activity in north-central United States: Evidence from varved lake sediments: Geology, v. 25, p. 331-334.

Dearing, J. (1994). Environmental magnetic susceptibility. Using the Bartington MS2 system. Kenilworth, Chi Publ.

Donner, S. D., & Kucharik, C. J. (2003). Evaluating the impacts of land management and climate variability on crop production and nitrate export across the Upper Mississippi Basin. Global Biogeochemical Cycles, 17(3).

Ellwood, B. B, Balsam, W. L, Roberts, H. H, (2006), Gulf of Mexico sediment sources and sediment transport trends from magnetic susceptibility measurements of surface samples, Marine geology, v. 230, pp 237-248.

Ellwood, B. B., Crick, R. E., El Hassani, A., Benoist, S., Young, R., 2000, Magneto susceptibility event and cyclostratigraphy (MSEC) in marine rocks and the question of detrital input versus carbonate productivity. Geology, 28, 1135-1138.

Farrel, K.M., 1987, Sedimentalogy and facies architecture of overbank deposits of the Mississippi River, False River Region. Louisiana. In Recent Developments in Fluvial Sedimentalogy (Ed. by F.G Ethridge, R.M Floresand M.D Harvey). Pp. 113-120.

Fisk, H.N., 1944, Geological Investigation of the Alluvial Valley of the Lower Mississippi River: US Army Corps of Engineers, Mississippi River Commission, Vicksburg, MS.

Frazier, D. E. (1967). Recent deltaic deposits of the Mississippi River: their development and chronology.

Gee, G.W., and Bauder, J.W., 1986, Particle-size analysis, *in* Klute, A., ed., Methods of soil analysis: Part 1: Physical and mineralogical methods, 3rd ed.: Madison, Wisconsin, Soil Science Society of America, p. 383–411.

Goolsby, D. A., Battaglin, W. A., Lawrence, G. B., Artz, R. S., Aulenbach, B. T., Hooper, R. P., ... & Stensland, G. J. (1999). Flux and sources of nutrients in the Mississippi-Atchafalaya River Basin: Topic 3 Report for the Integrated Assessment on Hypoxia in the Gulf of Mexico.

Goolsby, D.A and Battaglin, W.A., 2000, Nitrogen in the Mississippi basin-estimating sources and predicting flux to the Gulf of Mexico: USGS.

Guccione M.J., 1993, Grain-size distribution of overbank sediment and its use to locate channel positions. In: Alluvial sedimentation (Ed. by M. Marzo and C.Puigdefabregas), pp 185-194, Spec Pub. Int Ass. Sediment., 17.

Heitmuller, F. T., & Hudson, P. F. (2009). Downstream trends in sediment size and composition of channel-bed, bar, and bank deposits related to hydrologic and lithologic controls in the Llano River watershed, central Texas, USA. Geomorphology, 112(3), 246-260.

Heitmuller, F. T., Hudson, P. F., & Kesel, R. H. (2017). Overbank sedimentation from the historic AD 2011 flood along the Lower Mississippi River, USA. Geology, 45(2), 107-110.

Horowitz, A.J., 2010, A quarter century of declining suspended sediment fluxes in Mississippi River and the effect of the 1993 flood: Hydrological processes, v. 24, p. 13-34.

Hudson, P.F., and Kesel, R.H., 2000, Channel migration and meander-bend curvature in the lower Mississippi River prior to major human modification: Geology, v. 28, p. 531–534.

Hudson, P.F and Heitmuller, F.T., 2003, Local and watershed scale controls on the spatial variability of natural levee deposits in a large fine-grained floodplain: Lower Pancuo Basin, Mexico: Geomorphology, v. 56, p. 255-269.

Hudson, P.F, Middelkoop H, Stouthamer E. 2008. Flood management along the Lower Mississippi and Rhine Rivers (The Netherlands) and the continuum of geomorphic adjustment. Geomorphology 101: 209–236.

Johnsson, M. J., & Meade, R. H. (1990). Chemical weathering of fluvial sediments during alluvial storage: The Macuapanim Island point bar, Solimoes River, Brazil. Journal of Sedimentary Research, 60(6).

Kesel, R. H., Dunne, K. C., McDonald, R. C., Allison, K. R., & Spicer, B. E. (1974). Lateral erosion and overbank deposition on the Mississippi River in Louisiana caused by 1973 flooding. Geology, 2(9), 461-464.

Kesel, R.H., Yodis, E., McCraw, D., 1992. An approximation of the sediment budget of lower Mississippi River prior to major human modification. Earth Surface Processes and Landforms 17, P: 711 –722.

Kesel, R.H., 2003, Human modifications to the sediment regime of the lower Mississippi River flood plain, Geomorphology 56: 325–334.

Khalil, K., Mary, B., & Renault, P. (2004). Nitrous oxide production by nitrification and denitrification in soil aggregates as affected by O 2 concentration. Soil Biology and Biochemistry, 36(4), 687-699.

King, Sammy L., and Bobby D. Keeland. "Evaluation of reforestation in the lower Mississippi River alluvial valley." Restoration Ecology 7.4 (1999): 348-359.

Knox, J.C., 1996, Late Quaternary Upper Mississippi River alluvial episodes and their significance to the Lower Mississippi River system: Engineering Geology, v. 45, p. 263–285.

Knox, J.C.., 2007, The Mississippi River System, in Gupta. A., ed., Large Rivers: Geomorphology and management, p. 145–182.

Kolb, C. R. (1963). Sediments forming the bed and banks of the lower Mississippi River and their effect on river migration. Sedimentology, 2(3), 227-234.

Milliken, K. T., Anderson, J. B., & Rodriguez, A. B. (2008). A new composite Holocene sea-level curve for the northern Gulf of Mexico. Geological Society of America Special Papers, 443, 1-11.

Miranda, L. E. (2005). Fish assemblages in oxbow lakes relative to connectivity with the Mississippi River. Transactions of the American Fisheries Society, 134(6), 1480-1489.

Mitsch, W. J., Day Jr, J. W., Gilliam, J. W., Groffman, P. M., Hey, D. L., Randall, G. W., & Wang, N. (2001). Reducing Nitrogen Loading to the Gulf of Mexico from the Mississippi River Basin: Strategies to Counter a Persistent Ecological Problem: Ecotechnology—the use of natural ecosystems to solve environmental problems—should be a part of efforts to shrink the zone of hypoxia in the Gulf of Mexico. BioScience, 51(5), 373-388.

Meade, R.H., and Moody, J.A., 2010, Causes for the decline of suspended-sediment discharge in the Mississippi River system, 1940–2007: Hydrological Processes, v. 24, p. 35–49.

Nanson, G.C., Croke, J.C., 1992., Genetic classification of floodplains: Geomorphology, v. 4, p.459-486.

National Centers for Coastal Ocean Science Gulf of Mexico Hypoxia Assessment, (Revised 2017, May 05), Retrieved from "https://www.ncddc.noaa.gov/hypoxia"

Phelps, Q. E., Tripp, S. J., Herzog, D. P., & Garvey, J. E. (2015). Temporary connectivity: the relative benefits of large river floodplain inundation in the lower Mississippi River. Restoration Ecology, 23(1), 53-56.

Rabalais, N. N., Turner, R. E., Wiseman Jr, W. J., 2002, Gulf of Mexico Hypoxia, a.k.a. "The dead zone", Annual Review of Ecology and systematic, v. 33, pp. 235-263.

Sahrawat, K. L. (2003). Organic matter accumulation in submerged soils. Advances in Agronomy, 81, 169-201.

Saucier, R.T., (1994b), Geomorphology and Quaternary geologic history of the Lower Mississippi Valley: Volume 01, US Army Corps of Engineers, Mississippi River Commission, Vicksburg, MS, 1-364 pp.

Schramm, H.L., Cox, M.S., Tietjen, T.E., and Ezell, A.W., 2009, Nutrient dynamics in the lower Mississippi River floodplain: Comparing present and historic hydrologic conditions: Wetlands, v. 29, p. 476–487.

Schönbrunner, I. M., Preiner, S., & Hein, T. (2012). Impact of drying and re-flooding of sediment on phosphorus dynamics of river-floodplain systems. Science of the total environment, 432, 329-337.

Singhe, A.B., 1972, On the bedding in the natural-levee and point bar deposits of the Gomti River, Uttar Pradesh, India., Sedim. Geol, 7, P309-317.

Six, J., Elliott, E. T., Paustian, K., & Doran, J. W. (1998). Aggregation and soil organic matter accumulation in cultivated and native grassland soils. Soil Science Society of America Journal, 62(5), 1367-1377.

Smith, D. G. (1994). Glacial Lake McConnell: Paleogeography, age, duration, and associated river deltas, Mackenzie River basin, western Canada. Quaternary Science Reviews, 13(9-10), 829-843.

Smith, L.M., 1996, Fluvial geomorphic features of the Lower Mississippi alluvial valley: Engineering Geology, v. 45, p. 139–165.

Smith, L. M., & Winkley, B. R. (1996). The response of the Lower Mississippi River to river engineering. Engineering Geology, 45(1-4), 433-455.

Sparks, R.E., (1995), Need for Ecosystem Management of Large Rivers and their floodplains. BioScience, 45 (3), 162-182

Teller, J.T. Proglacial lakes and the southern margin of the Laurentide Ice Sheet, In: North America and Adjacent Oceans during the Last Deglaciation, Eds, Ruddiman, W.F and Wright Jr, H.E, The Geology of North America. V, K3, p. 39–69.

Tockner, K., & Stanford, J. A. (2002). Riverine flood plains: present state and future trends. Environmental conservation, 29(03), 308-330.

U.S Fish and Wildlife Service, St Catherine Creek, (last updated on June 17, 2014), retrieved from, https://www.fws.gov/refuge/St_Catherine_Creek/about.html.

Ward, J. V and Stanford, J. A. (1995). Ecological connectivity in alluvial river ecosystems and its disruption by flow regulation. Regulated Rivers: Research & Management, 11(1), 105-119.

Wasklewicz, T.A., Grubaugh, J., Franklin, S., and Gruelich, S., 2004, 20th century stage trends along the Mississippi River: Physical Geography, v. 25, p. 208–224.

Wendland, W.M., 1996, Climate changes: impacts on geomorphic processes: Engineering Geology, v. 45, p. 347–358.

Zehetner, F., Lair, G. J., & Gerzabek, M. H. (2009). Rapid carbon accretion and organic matter pool stabilization in riverine floodplain soils. Global Biogeochemical Cycles, 23(4).

Zeug, S. C., & Winemiller, K. O. (2008). Relationships between hydrology, spatial heterogeneity, and fish recruitment dynamics in a temperate floodplain river. River Research and Applications, 24(1), 90-102.